Politecnico di Torino

Master degree in Energy and Nuclear Engineering, Renewable Energy Systems
A.a. 2021/2022
Sessione di Laurea Giugno 2023

Optimization of the spatial disposition of an array of floating offshore wind turbines using a Python genetic algorithm

Relatore: Prof. Sirigu Sergej Antonello
Co-relatore: Prof. Faraggiana Emilio

Candidato: Ferrari Ruggero, 288214

Contents

List of Figures

Abstract

Electricity has a social value as well as a monetary one, which is constantly increasing. It is a strategic asset that has become indispensable for years. For this reason, the energy production sector is fundamental, as is sustainable production, given the ongoing climate change.

The aim of this study is to optimize the spatial arrangement of an off-shore floating wind turbine array in such a way as to increase the efficiency and maximize the energy yield in relation to the cost of the initial investment.

The problem was tackled by combining two different analyses: an aerodynamics one and an optimization one.
The first one allowed to simulate the aerodynamic interactions between the turbines and the wind speed field, using analytical relations such as the Jensen model and the *Bastankhah Gaussian model* for the calculation of the wakes, accompanied by models for the calculation of the blockage effect, models for the turbulence, to simulate the ground effect or to model the rotors. The use of such models avoided using complex fluid dynamics simulation methods such as *CFD*, allowing to reduce the computational costs and enabling the use of heuristic optimization algorithms.
The second one, indeed, allowed to find the optimal arrangement of the turbines by means of a genetic algorithm that selected the best individual from generation to generation, that is, the disposition with the best performance.
To perform these calculations, two different Python libraries were used: PyWake for the aerodynamic calculations, and Pymoo for the evolutionary algorithm.

The investigation did not limit itself to an analysis of producibility but also considered economic aspects of the investment.
The results show the existence of an optimal number of wind turbines to be inserted in a specific domain. They also show that for the case study, the arrangement is strongly influenced by the dominant wind direction. The algorithm proved to be stable and convergent.

This thesis contributes to provide solutions for the design of wind farms by suggesting a synthesis between accuracy of results and computational intensity.

1 Introduction

This work aims to investigate the optimal layout for an array of floating off-shore wind turbines.

An optimized layout is crucial to maximize the energy production and reduce the waste of resources and, above all, maximize the convenience. The wind turbines can interfere with each other. In fact, by converting the wind speed into rotational kinetic energy, they disturb the wind speed field, reducing it. This effect modifies the air column behind it in a phenomenon called wake effect. It can be understood how a turbine that encounters wake wind and not undisturbed wind has a deficit because the wind with which it interfaces is slower. Optimizing the layout of an array of wind turbines means reducing the shadowing effect as much as possible. This phenomenon is more complicated when viewed in three dimensions.The aforementioned criterion, in fact, must be considered for every possible direction of the wind. Therefore, a configuration that could be perfect for one direction, could be subject to powerful wake effects for another.

However, it is not enough to place the wind turbines at kilometric distances from each other. At the same time, in fact, it is necessary to adopt configurations that are as compact as possible to avoid wasting space useful for the production of electricity. The latter necessity is mainly imposed by economic considerations that, however, cannot be ignored and indeed, guide the decision-making processes more than considerations of producibility.

A crucial parameter to evaluate a power generation plant is the cost that is necessary to sustain to produce a unit of energy; the lower it is, the better. In a plant where the resource has no costs, the most important source of expenditure is the initial investment. It consists of many items, among which the cost of the electrical cables that depends on its length, whose price, being medium-voltage submarine cables, is anything but negligible. Therefore, the closer the turbines are, the lower the initial investment and therefore the cost of energy production.

Having to reconcile these two opposite behaviors makes the analysis complex and articulated. And that is why it is necessary to analyze a range of possible solutions that is as wide as possible. Therefore, it is excluded to be able to perform the analysis of the wake effects and in general of the wind speed field in the wind-farm with high-fidelity methods with prohibitive computational costs such as Computation Fluid Dynamics analysis. Consequently, more rapid and consequently approximate methods, called analytical models, will be chosen, thanks to which it will be possible to evaluate a much higher number of solutions. This allows the use of innovative optimization methods such as heuristic algorithms.

A heuristic optimization algorithm is a stochastic algorithm that relies on random procedures for the search of global maximum or minimum points of the functions to be optimized.

By proceeding randomly, it is possible to cover an extremely wide range of possible combinations. However, only by increasing the number of combinations processed, the precision and reliability of the result are increased. Precisely because it is necessary to process a very high number of combinations, the optimization algorithm cannot be combined with methods of evaluating the aerodynamic field with high computational intensity.

A genetic evolution algorithm will be used to perform the optimization of the layout. It generates a series of arrays by randomly arranging the wind turbines in the plane. It will identify each layout as individuals and the group just generated, as generation. It will evaluate the producibility of each layout, that is, of each individual, with the already mentioned analytical models and with it the cost of energy production. For each generation, best individuals are evaluated based on which, by crossing their characteristics as in genetic reproduction, the next generation is produced. The succession of generations and the selection of the best individuals leads to an evolution of the population of individuals that brings the best layout closer and closer to the optimized layout.

In conclusion, the combined provision of genetic algorithm and analytical models of aerodynamic evaluation aims to provide a fast and generalizing optimization method, which is able to identify the optimal configuration precisely because the speed with which the evaluations are carried out allows to examine a number of possible solutions extremely large.

The thesis is divided into several chapters. Initially, the **energy outlooks** will be analyzed with a broad-spectrum approach, in time and space, analyzing historical trends and future prospects for different areas in the world, with an overview of the technologies available today and a focus on wind turbines.
Subsequently, the **State of the art of the design methods** and optimization of wind power plants will be analyzed. The mathematical models commonly used for aerodynamics calculations for turbine interactions will be presented.
In the next chapter, **The algorithm** will be presented, where all the assumptions and decisions that have been made to perform the calculations will be discussed. The composition of the evolutionary optimization algorithm and the chosen aerodynamic calculation model will be articulated in detail, discussing the sub-models of which they are composed and justifying their choice.
Finally, the **results obtained** will be presented and analyzed. The analyses performed, the expected and achieved results will be discussed with a critical eye.
The **conclusion** chapter will retrace the entire thesis with a more aware approach on the results achieved, being able to give a global interpretation with a posthumous approach.

2 Energy outlook

"Climate change is the central challenge of our century", as stated by the United Nations Secretary-General António Guterres on the occasion of $COP - 27$ in Sharm el-Sheik
This is a phenomenon that has disastrous implications of global scope, which require an urgent and coordinated response from the international community. However, climate change is not only a threat, but also an economic opportunity. In fact, the ecological transition that is taking place represents a potential driver of growth and innovation for the countries and businesses that will be able to seize it.
Investments in the ecological transition are constantly increasing. In 2022 they reached a value of 1.1 trillion dollars at the global level. [1] Moreover, estimates predict that this market could produce 395 million jobs by 2030 and add up to $10.1 trillion in annual business value [2].

The ecological transition involves all the main sectors responsible for climate change, which are those that generate CO2 emissions from human activity. Starting from agriculture and livestock, reaching the transport and energy sector. This is one of the most focused sectors, not only because it causes one of the largest portions of greenhouse gas emissions, but also because it is among the most suitable to undergo a transition.

At the global level, emissions are divided into 6.4% for housing, 14% for the transport sector, 21% for industry, 24% for AFOLU and 25% for the sector for energy and heat production [3].
The latter is a centralized sector, at least the portion with high carbon intensity and this allows to carry out targeted investments with quick results. On the contrary, for example, to reduce the environmental impact of the domestic sector it is necessary to promote policies of renewal and efficiency of buildings and boilers through incentives or tax breaks and this has a more diluted impact over time.
In any case, the ecological transition wants to touch all the sectors discussed so far and although one of the protagonists, the renewal of the energy sector is only a part of a larger project. However, given the topic of this thesis, this chapter will specifically analyze only the latter.

It is in the context just described that the trends and prospects of the energy landscape at the global, European and Italian level must be analyzed. Without neglecting, of course, those of the major greenhouse gas emitting countries such as the united States and China. Moreover, the countries of the third world that are experiencing a dizzying population growth must not be ignored. Indeed, it is not possible to interpret and therefore manage correctly the context of the energy sector without talking about demography, climate emergency, social inequality, national security, economic crisis, infrastructure and geopolitics. Moreover, it is necessary to understand what the future scenarios will be in order to understand what roles renewable energies will have in light of the issues discussed up to this point.

For what has been said so far, this chapter will analyze in the first place the **World, Europe and Italy energy portfolio and scenario** by performing an analysis of the historical trends for different geographical areas. Based on these, possible future Energy scenarios will be outlined with demographic or geopolitical considerations. The effects of European regulations for Europe itself will be explored, with particular interest for Italy.
Finally, we will discuss the **renewable energy role** in the process of the green revolution. Specifically, we will talk about wind energy, with particular attention to offshore wind. The chapter will conclude by deepening the floating offshore wind and presenting its state of the art, characteristics, advantages and disadvantages.

2.1 World-Europe-Italy energy portfolio and scenario

The energy sector has undergone a profound transformation since the Industrial Revolution, when coal and oil replaced wood as the main sources of energy for heating, lighting and mobility. During the XX century, other sources of energy were also developed, such as nuclear energy and renewable energies, which presented different advantages and challenges compared to fossil fuels.

Since the $90s$, the world's electricity consumption has more than doubled.[4] Most of this growth has been driven by emerging countries, especially China and India, which have increased their demand for electricity to support economic and social development.

Europe has been one of the most active regions in the energy transition towards cleaner and more diversified sources. Since the same years, the European Union has adopted a series of directives and strategies to liberalize the internal energy market, promote renewable energies and energy efficiency, reduce greenhouse gas emissions and ensure energy security.

Italy has followed the European developments in the energy sector, adapting its legislation and promoting incentive policies for renewable sources. The energy market in Italy was liberalized starting from 1999. Italy has also increased its share of renewable energies in electricity production, however it remains a resource-poor country that self-produces only a minimal part of the energy it needs.

However, despite the strong increase of renewable energies, which reached a historical milestone in 2021 when the generation of electricity from renewable sources exceeded the share produced by coal,[5] the global electricity mix is still dominated by fossil fuels, which account for 62% of the total. [6] The production from fossil sources is not decreasing, and the increase in the share of renewables is barely enough to cover the increase in electricity demand.[7] This increase is mainly caused by the growth of Chinese demand. The data show increases in electricity demand in 2021 in almost all states, including those in Europe.[8] But they are affected by the disturbances due to Covid-19. Looking at the pre-Covid data of 2019, it turns out that China is the one that increases the demand for electricity most, against a context in which Europe and the USA even reduce it. The Chinese electricity demand remains high, showing no signs of decreasing, and stands at 25%. As a consequence, the per capita energy demand also increases, which in 2021 is higher than the consumption in the UK. [9].

China is one of the main players in the fight against climate change. So are the United States, which rank second in total energy consumption with $2123 Mtoe$ in 2021. [10] And with one of the highest per capita energy consumption. However, they are not an emerging country.

To deepen the situation at the global level, we should also consider the areas with the highest population growth. This will indeed determine the future trends, both in terms of energy demand and environmental impact.
India and Africa should be mentioned above all, which together host almost 40% of the world population and produce less than 10% of the global carbon dioxide emissions. [11], [12], [13]
It is expected that these regions with large prospects of economic and social growth will also experience a huge increase in the production of climate-altering substances. For this reason, it is important to support their development with policies of cooperation and solidarity, that limit the low-cost development, typically by means of fossils, and favor the ecological transition and the diversified responsibility. This means encouraging the use of renewable energies, the efficient management of natural resources, the protection of biodiversity and the reduction of energy poverty. [14]

Europe has committed to achieving climate neutrality by 2050, i.e. to emit only what can be absorbed by the environment. To do so, it has adopted a series of rules and policy initiatives within the framework of the European Green Deal. [15]
Among the main measures is the European climate law, which sets a binding EU climate target for a net reduction of greenhouse gas emissions (emissions net of absorptions) of at least 55% by 2030 compared to 1990 levels with a measure called *Fit for* 55.[16]. This package includes cross-sectoral measures on many sectors, among others, the revision of the EU emissions trading system (ETS), the renewable energy directive and the energy efficiency directive, the regulation on land use and forestry and the regulation on CO2 emissions from cars and vans.

Specifically, we can mention the reform of the ETS, which provides for the extension of the system to the maritime sector, the creation of a new system for fuels for heating and transport and a faster reduction of the number of available allowances[16]. Moreover, there is the revision of the renewable energy directive, which sets a binding EU target of 40% of energy from renewable sources in final energy consumption by 2030 and introduces new rules to foster the development of renewable sources in the electricity, heating and transport sectors[17].
The measure also revises the energy efficiency directive, which sets a binding EU target of 39% reduction in primary energy consumption and 36% reduction in final energy consumption by 2030 and introduces new measures to improve the energy efficiency of buildings, products and services[18]. It revises the energy taxation directive, which proposes to adjust the minimum rates of excise duties on energy products according to their energy content and their CO2 emissions, in order to discourage the consumption of fossil fuels and encourage that of renewable sources[16].
A promising novelty is the introduction of a carbon border adjustment mechanism (CBAM), which provides for the application of a tax on imports of certain products from countries with less ambitious climate standards than the EU, in order to avoid the relocation of emissions and unfair competition[19]. The products concerned are cement, iron, steel, aluminium, fertilisers, electricity and hydrogen. Importers will have to buy carbon credits based on the carbon price they would have had to pay if the products had been produced in the EU. [19]

All this is also reflected at the Italian level in measures and changes dictated also by the exploitation of the funds of the National Recovery and Resilience Plan (PNRR) which provides for resources for 40.3 billion euros for the component "Renewable energy, hydrogen, network and sustainable mobility", with the aim of increasing the share of energy from renewable sources in gross final consumption to 30% by 2026 and to 40% by 2030. [20]
Italy has also increased its share of renewable energy in electricity production, which rose from 16% to 40% between 1990 and 2019. [21] However, in the same period emissions were reduced by only 19%. [22] Therefore, it is evident that other measures and investments are necessary to meet the objectives set by the European plans.

The actions taken by Italy and the European Union are in line with the scenarios of the IPCC, the Intergovernmental Panel on Climate Change, which explores the possible trajectories of mitigation and adaptation to global warming. The scenarios are based on different levels of radiative forcing (RF), which measures the net effect of greenhouse gases and aerosols on the Earth's energy balance. The scenarios range from the most optimistic ones (RF below $2.6W/m^2$ by 2100), which imply a strong reduction of emissions and a possible achievement of climate neutrality by mid-century, to the most pessimistic ones (RF above $8.5W/m^2$ by 2100), which foresee an increase of emissions and an average warming above $4°C$ compared to pre-industrial levels. [23]
The most likely scenario is the intermediate one (RF between 2.6 and $3W/m^2$ by 2100), which

requires a reduction of emissions by 45% by 2030 and by 100% by 2050 compared to 2010, to limit warming to $1.5°C$ with a 50% probability. This scenario entails a rapid and widespread transition towards an energy system based on renewable sources, which should cover 85% of electricity production and 65% of final energy consumption by 2050. [24]
In any case, with each of them the role of renewable energy is essential, as it allows to reduce the dependence on fossil fuels, to diversify the energy mix, to create employment and innovation, to improve energy security and to contribute to the fight against climate change.

The main renewable sources of electricity are hydroelectric, wind and solar. In 2021, these sources accounted for significant shares of global renewable electricity production: about $4,273TWh$ (54%) were hydroelectric energy, $1,862TWh$ (23%) were produced by wind and about $1,033TWh$ (13%) by solar. [25]. The other renewable sources, such as biomass, geothermal, wave and tidal, contributed for 8%. [26]

2.2 Renewable energy role

At the global level, renewable energy recorded a record growth in 2021, reaching an installed capacity of over $3,100GW$, with an increase of 17% compared to the previous year. However, the overall share in final energy consumption remained stagnant, due to the strong increase in demand and the recourse to fossil fuels to cope with the energy crisis. [27]

In any case, renewable energy sources recorded a strong growth in 2021. According to the data published by IRENA, among the different technologies, hydroelectric power reached an installed capacity of about $1,330GW$, with an increase of 12% compared to 2020, contributing to avoid the emission of about 2,800 million tons of CO2 into the atmosphere. [28]
Photovoltaic followed an even more positive trend, with a 23% growth in installed capacity, which reached $789GW$. This source allowed to reduce CO2 emissions by about 1,300 million tons. [28]
Wind power has maintained an important role in the energy transition, representing 26% of the new renewable capacity installed in the world in 2021. The total wind capacity reached $733GW$, with an increase of 18% compared to 2020. Thanks to this technology, about 1.2 billion tons of CO2 were avoided in the atmosphere.[28]

Wind power has several characteristics that make it one of the most valid alternatives among renewable energy sources. One of these is the fact that it has costs per unit of energy that are increasingly competitive with those of fossil fuels and can exploit areas that are not suitable for agriculture or construction. Moreover, wind power has a high energy efficiency, as it can produce energy even at night or in conditions of low brightness. For this reason, it is an energy source that is receiving more and more attention and investment from governments and companies, as it contributes to the transition towards a cleaner and more sustainable energy system.
In any case, the biggest advantage of wind power is its scalability.
The larger the turbines are, the more they capture the wind and the more they produce energy. Modern wind turbines can reach diameters of over 200 meters and heights of over 250 meters. [29] This entails a lower environmental and visual impact. Larger wind turbines can be installed at greater distances from each other, reducing noise, shading and the effect on flying fauna. [30] But also a higher production of electricity per unit of occupied area. A $10MW$ wind turbine could produce the same energy as 10 turbines of $1MW$, but occupying less space. A higher reliability

and durability. Larger wind turbines are designed to withstand more extreme weather conditions and have a longer lifespan. [30]
And offshore wind is even more promising than onshore wind.

Offshore wind, in fact, benefits from the large dimensions typical of the open sea, which further favor the scalability discussed above. Moreover, the wind at sea is stronger, more constant and predictable, therefore, having a higher producibility, it allows to install even larger and more powerful turbines. Finally, the wide sea surface available offers many opportunities for locating wind farms, further reducing the wake effects and favoring efficiency.

The advantages that distinguish offshore installations from onshore ones can be further increased by floating technologies, which allow to exploit the wind in deep waters where it is not possible to install turbines with fixed foundations. Floating technologies offer greater flexibility and adaptability to different weather and sea conditions in choosing the locations of wind farms, which can be moved according to needs.[31] As well as the possibility of exploiting the wind in deep waters where it is not possible to fix the turbines to the seabed.[32], [31]
Moreover, they reduce the construction and installation costs of the turbines, which can be assembled on land and then towed to sea.[32]
Finally, they involve less interference with maritime activities and marine biodiversity.

Floating wind is a technology still in development, but it has a great potential for growth. According to some studies, the installed capacity of floating wind in the world could reach $289GW$ by 2050. [32]

Figure 1: Floating wind turbine models, *Image by Josh Bauer, NREL*

Among the different technologies for floating, three main models can be distinguished, visible in

fig. 1: the spar, the semi-submersible platform and the tension-leg platform. Each of these models has pros and cons, which must be evaluated according to the characteristics of the site and the project.

The spar is a long cylindrical structure that extends deep below the water surface and is stabilized by a counterweight. This model offers good stability and resistance to waves, but requires a minimum depth of 100 meters and involves difficulties in transport and installation. [32]

The semi-submersible platform is a structure with several columns that rest on floats and are connected by beams. This model offers good flexibility and adaptability to different depths and weather and sea conditions, but is more exposed to waves and wind and requires more maintenance. [32]

The tension-leg platform is a structure with one or more columns that are anchored to the seabed with tensioned cables. This model offers low exposure to waves and wind and requires less maintenance, but requires a minimum depth of 50 meters and is more complex to design and install. [32]

Each technology has advantages and disadvantages in terms of costs, performance, stability and environmental impact. The choice of technology may depend on several factors, such as water depth, wind speed, weather and sea conditions and transport and installation needs.
For the work of this thesis we will choose the spar buoy model as one of the simplest and most common.

3 State of the art of the design methods

In engineering, there are numerous simulation models that allow for optimal design of a wind farm. These models can deal with the simulation of the wind speed map in the wind farm through the utilization of the **wake deficit effect models**, or with its **optimization algorithm**.

3.1 Wake deficit effect models

The simulation of the wind speed field mainly consists of evaluating the wake effects of the turbines and assessing their impact on the performance of the turbines themselves and of the wind farm in general. The most impactful wake effects are the reduction of the wind speed downstream of the turbines, the deviation of its direction and the increase of turbulence.
As we will see later in section 4.2 there are many factors, and therefore models that contribute to the calculation of the wind speed map. However, the main model that tends to determine the accuracy and the computational cost of the analysis is the model for the simulation of the wake effects.

The calculation of the wake downstream of the wind turbines can be performed with very different models. Starting from the most accurate ones, which take into account the geometry of the blades, the rotation speed, the direction and intensity of the incoming wind, the atmospheric turbulence and the interactions between the turbines. And arriving at the most approximate ones, which assume the wake as a cone with a constant expansion angle.

3.1.1 Computational Fluid Dynamic, (*CFD*) method

Fluid dynamics computation evaluate the wind flow around the wind turbines and the wake velocity field by solving numerically the Navier-Stokes equations that describe those phenomena.
This method is very accurate but requires many computational calculations and resources.

The basic equations that describe the dynamics of fluids are the eq. (1); Navier–Stokes in vector form. [33]

$$\rho\left(\frac{\partial \mathbf{v}}{\partial t} + \mathbf{v}\cdot\nabla\mathbf{v}\right) = -\nabla p + \mu\nabla^2\mathbf{v} + \mathbf{f} \tag{1}$$

They are differential equations without an analytical solution. Therefore, to solve them, it is necessary to introduce simplifications or approximations. The main calculation models for approximating these equations introduce hypotheses according to which the differential equations become linear. Among the main methods of spatial approximation there are: finite difference method, finite element method and finite volume method. These methods require dividing the domain into small cells or elements creating a mesh of points, on which the mathematical model is applied under the hypothesis of linearity of the solution for each cell; that is, of the fields of velocity, pressure and temperature.
Euler's explicit or implicit method can be used for temporal approximation.

This type of discretization involves, as mentioned, the introduction of approximations. However, the error introduced is reduced by increasing the points in which the domain is divided and therefore by increasing the operations of evaluating the solution. This means that with *CFD* methods it is possible to obtain solutions extremely faithful to reality. However, at the expense, of computational costs, which become extremely high due to the use of very dense meshes.

3.1.2 *CFD* Wake Modelling with a *BEM*,(Blade Element Momentum)Wind Turbine Sub-Model

This method combines *CFD* calculations to analyze the velocity field with the blade element momentum theory to model the rotor.

"Modelling of wind farms using computational fluid dynamics (*CFD*) resolving the flow field around each wind turbine's blades on a moving computational grid is still too costly and time consuming in terms of computational capacity and effort. One strategy is to use sub-models for the wind turbines, to handle interaction of wakes in wind farms" [34].
Blade element momentum theory combines the blade element theory and momentum theory. It is able to calculate the local forces on wind-turbine blade simplifying the *CFD* computational cost.
By the *BEM* theory the tangential and normal forces acting on the wind turbine blades are computed. These forces are distributed as reaction forces on the rotor plane. They will be added as sources in the conservation of momentum.

The *BEM* theory can be used to relate blade shape to the rotor's ability to extract power from the wind.
This theory assumes two-dimensional geometries, therefore introduces errors. It is less accurate but faster than classic *CFD* method.

3.1.3 Large Eddy Simulation

Is a mathematical model for the simulation of turbulent flows by numerically solving the Navier–Stokes equations used in computational fluid dynamics.
The basic concept of this method is to reduce the computational cost of the analysis by applying the Navier-Stokes equations in a space described in a discrete and finite way.
Therefore I apply a spatial filter to the original Navier-Stokes equations, in order to solve only the largest turbulent structures and neglect the smaller structures in a more optimized way.

Filters can be implicit or explicit. Explicit filters reduce the truncation error but require a finer grid, thus the computational cost increases.

The Large Eddy Simulation is therefore a model that takes into account the instantaneous turbulence and the meandering of the wake, but not the sub-grid turbulence. It also requires a model for the aerodynamic forces on the turbine blades, which, for example, can be based on the already seen *BEM* theory.

Also in this case the computational costs are extremely relevant and inaccessible for the kind of analysis in combination with an optimization algorithm, in objective to this thesis.[35], [36]

3.1.4 Reynolds-averaged Navier–Stokes, (RANS) method

The *RANS* is a method to solve fluid dynamic problems. It solves the Navier-Stokes equations averaged in time over a particular time span, small compared to the phenomenon to be simulated, large compared to the turbulent phenomena.
The *RANS* can be defined as a wake deficit model that takes into account the average turbulence, but not the instantaneous turbulence or the wake meandering.[37]

This method is a cost-effective and widely used method for simulating turbulent flows. It can also be applied to complex geometries, but it is not suitable for all phenomena; for example, it is not accurate for simulations with flow separation.
Nevertheless, it is extensively used for internal and external flows over aerodynamic bodies and with heat transfer.
The RANS has a lower fidelity than the Large Eddy Simulation, but also a lower computational cost.[38]

3.1.5 Jensen model

The Jensen model is an analytical model to valuate the wake effect, among the simplest and with less computational effort.
it is based on the principle of conservation of momentum. It simulates the wake as a cone with a constant expansion angle according to eq. (2) and the equation to describe the thrust coefficient reported in section 4.2.3.[39], [40]

$$u = \left[1 - \frac{2a}{1 + \alpha(x/r_d)^2}\right] U_\infty \tag{2}$$

Dove:

- $r_d = r_{WT}\sqrt{\frac{1-a}{1-2a}}$; is the equivalent downstream rotor radius [41]
- r_{WT}; is the radius of the wind turbine.
- a; is the induction factor.
- x; is the distance between two turbines.
- α; is the wake entrainment constant, also known as the wake decay constant.
- U_∞; is the free wind speed.

In fig. 2 it can be seen d and r_d that is the half of D_d. [41]

Studies compare it with other more accurate methods and it results that the Jensen model is sufficiently faithful to the real results if one considers that it solves a single equation. [39], [42]

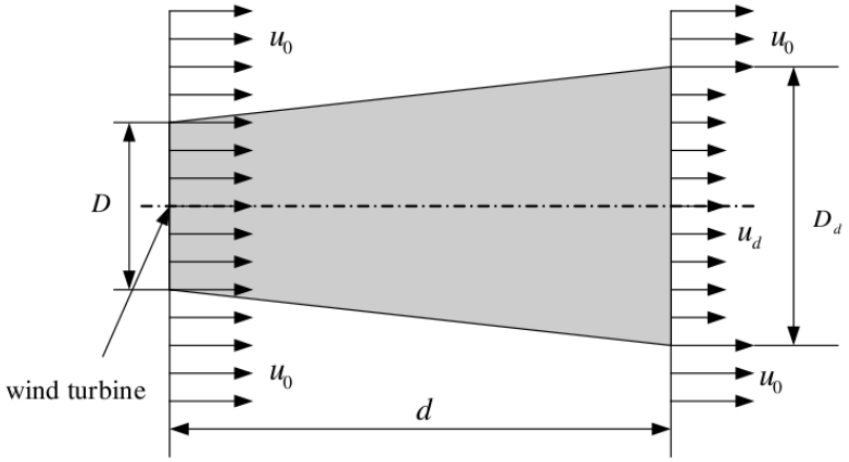

Figure 2: Momentum conservation on a wind turbine

3.1.6 Bastankhah Gaussian Model

The Bastankhah Gaussian Model is an analytical model for calculating the wake effect.
While the already seen Jensen model assumes a constant expansion conical shape for the velocity deficit in the wake, the Bastankhah Gaussian model assumes a Gaussian shape. That is, the wake effect is maximum on the wake axis and decreases exponentially towards the outside. This shape is more realistic than the cone of the Jensen model because it takes into account the diffusion of the wake due to turbulence and viscosity. Therefore, the Jensen model will have a discontinuity in the velocity profile at the edge of the wake, while the Bastankhah Gaussian model has a more gradual transition.[43]

Moreover, the Jensen model does not take into account the effects of wake rotation, viscosity and atmospheric stability on the velocity deficit. The Bastankhah Gaussian model instead considers them and incorporates them into the parameter k^* and the correction factor β. The model uses the eq. (3). [44]

$$\frac{\Delta U}{U_\infty} = \left(1 - \sqrt{1 - \frac{C_T}{8(k^* x/d_0 + 0.2\sqrt{\beta})^2}}\right) \exp\left(-\frac{C_T}{2(k^* x/d_0 + 0.2\sqrt{\beta})^2}\left[\left(\frac{z - z_h}{d_0}\right)^2 + \left(\frac{y}{d_0}\right)^2\right]\right) \tag{3}$$

Where:

- Δu; is the wake velocity deficit
- u_∞; is the free wind speed.
- x; is the downstream distance.
- d_0; is the rotor diameter and the diameter of the wake on the rotor.
- $\beta = \frac{1}{2}\frac{1+\sqrt{1-C_T}}{\sqrt{1-C_T}}$; is a parameter that depends on the thrust coefficient.
- k^*; is the growth rate of the wake.

- C_T; is the thrust coefficient of the turbine.
- y and z; are the lateral and vertical coordinates, respectively.
- z_h; is the axis height of the turbine.

Therefore, this last model is more faithful to reality, albeit with a higher computational cost.
Finally, it should be considered that "the model is valid in the far wake only"[43].

In the calculations of this work, the choice of wake models will fall on the last two presented. The main reason is their computational cost.
By integrating the aerodynamic calculations of wind farms with a metaheuristic optimizer, as discussed in the next section, the use of wake models becomes intensive and no longer compatible with *CFD* calculations that would make the calculation times prohibitive.

3.2 Optimization algorithm

In the analysis under consideration for this thesis, the objective functions to be optimized are very complex. They depends on the position of the turbines in a very complex way and can vary a lot with small variations of the coordinates. Therefore, the problem is non-linear and potentially discontinuous. Moreover, the objective function is not known in analytical form and the search space is very large with a wind speed field that varies depending on the wake effects of the various turbines.
Finally, it must be considered that we want to find a global solution or at most as close as possible to the global one. And not all algorithms can guarantee this.

For problems of this complexity, we chose to use metaheuristic optimization algorithms.
Metaheuristic algorithms are computational methods that are “meta”, beyond, and “heuristic”, based on empirical or intuitive rules; that is, beyond deductive rules.

They try to optimize a problem iteratively, starting from a candidate solution and trying to improve it according to a certain measure of quality.
Metaheuristic algorithms do not make any specific assumptions about the problem to be optimized and can explore very large spaces of possible solutions. However, they do not guarantee to find the optimal solution.
Many of those algorithms are based on empirical or intuitive rules that work well in practice, but do not have a rigorous theoretical justification. They are generally very effective and adaptable to the problem. However, they take a long time to converge.

Some examples of metaheuristic algorithms are Simulated annealing, Tabu search, Evolutionary algorithms, Neural networks or Ant systems. These algorithms are inspired by many different types of natural processes.

- *Neural network*; it is inspired by the functioning of the human brain based on learning from input and output data.

  It consists of artificial neurons connected by synaptic weights, which transmit and transform signals according to an activation function. A neural network can have different layers: input, output and hidden. The training of the network occurs through algorithms that modify the weights based on the error made. Neural networks have the advantage of being able to classify complex and non-linear patterns, work in parallel, tolerate errors and noise

and achieve high accuracy. However, they also present some challenges, such as the choice of parameters and components of the network, which requires empirical experimentation, and the high computational and temporal cost for the training and validation of the network.

They are algorithms particularly suited for applications where it is necessary to learn from large amounts of unstructured or noisy data, and adapt to changes in the environment to provide fast and effective answers.[45]

- *Simulated annealing*; it minimize an energy function by accepting also worsening moves with a certain probability that decreases with the temperature.[46]

  Particularly suitable if the problem has a continuous and differentiable objective function. [47]

- *ant colony algorithm*; is based on the behavior of ants.

  They are algorithms based on autonomous agents that communicate with each other through pheromone traces deposited on the followed path.
  Suitable for combinatorial optimization or routing problems such as the traveling salesman problem.[48]

- *Tabu search*; it uses a short-term memory to avoid returning to the solutions already visited and to allow worsening moves.[46]

  They are to be used specifically for problems with a discrete or combinatorial objective function.[49]

- *Evolutionary algorithms*; they are based on the principle of biological evolution, which consists in modifying a population of candidate solutions through mechanisms such as reproduction, mutation, recombination and selection.[46]

  Its functioning is inspired by the natural processes that lead to the formation of species adapted to their environment.

  They are algorithms with the ability to solve complex, nonlinear, multimodal or constrained problems and to explore the solution space in a diversified and creative way. They have a remarkable robustness to errors and noise, thanks to the redundancy and variability of the population.
  They are also flexible and adaptable to different types of problems and representations.
  However, there is a considerable difficulty in choosing the parameters and genetic operators, which greatly influence the performance and require empirical experimentation. Moreover, they run the risk of stagnation or premature convergence to suboptimal or local solutions.
  Finally, they have a high computational and temporal cost for the evolution of the population, especially for problems of great size or complexity.[50]

As presented at the beginning of the chapter, since the nature of the problem addressed in this work coincides with the characteristics of the latter family, the choice of the optimization algorithm will fall on an evolutionary algorithm despite the not negligible defects.

3.2.1 Evolutionary algorithm

As already introduced, evolutionary metaheuristic algorithms are algorithms that are inspired by the mechanisms of natural selection and genetics to find approximate solutions to complex optimization problems.

Such algorithms operate on a population of candidate solutions, called individuals, that represent possible answers to the problem to be solved. Each individual has a genotype, that is a coding of its characteristics, and a phenotype, that is the value of the objective function associated with the solution.
Evolutionary algorithms apply mutation and recombination operators to the genotypes of the individuals, generating new solutions that can be better or worse than the previous ones. These operators introduce variation and diversity in the population, exploring the solution space. And they use a selection criterion to choose which individuals survive and which are discarded, based on their phenotype. This criterion favors the solutions that are more suited to the problem, that is those that optimize the objective function.

An evolutionary algorithm consists of four main phases: initialization, evaluation, variation and selection. In the initialization phase, a initial population of random or heuristic solutions is generated. In the evaluation phase, the quality of the solutions is calculated by a fitness or merit function. In the variation phase, genetic operators such as crossover and mutation are applied to create new solutions from the existing ones. In the selection phase, the solutions to keep in the population are chosen based on their fitness or other criteria.

An example of evolutionary algorithm is the *NSGA-II* (Non-dominated Sorting Genetic Algorithm) that is a multi-objective evolutionary algorithm that allows to optimize multiple functions simultaneously finding the best trade-off. The selection criterion used by this algorithm is that of non-dominance that defines a partial preference relation between two multi-objective solutions. A solution x dominates a solution y if x is better or equal to y in at least one objective. A solution x is non-dominated if there is no other solution that dominates it. *NSGA-II* uses non-dominance to sort the solutions into different fronts, where the first front contains the non-dominated solutions, the second front contains the solutions dominated only by the first front, and so on.[51]

Another possible evolutionary algorithm is the single objective genetic one.
The main difference between NSGAii and GA is that the former is a multiobjective, while the latter is a single-objective algorithm. This means that NSGAii tries to optimize multiple objectives simultaneously, while GA tries to optimize only one objective.[50]

Later it will be seen that, given the contingencies of the problem, we will opt for adopting the single-objective genetic resolution.

4 The algorithm

As mentioned earlier, the aim of this work is to optimise the arrangement of a set of wind turbines by creating generations of individuals and selecting the best ones to create the next generation based on their characteristics.
In the context of this work, the individual corresponds to the single specific arrangement of the array (x and y coordinates of all turbines that make up the array), while the generation is a group of individuals. The quality of the individuals is evaluated based on the performances obtained by simulating the aerodynamic field of each of them.
That is, I make a selection, generation by generation, of individuals, that is, of arrangements of aerogenerators. Whereby the evaluation is done by distinguishing the determinations according to their performance.

This definition of the problem is still very general, because the optimisation must be carried out according to a certain parameter, or at least the purpose must be defined.
An array of wind generators can be optimised to minimise the area occupied or the investment cost, or perhaps even to maximise the energy generated or to reduce the cost. And all these would be appropriate studies. However, for a conscious analysis, it is good to look at the results of all the studies together, without committing to a single objective and disregarding the others. To avoid this mistake, we will not proceed with a single objective in the analysis, but choose unanimously between them.
For example, if we were to consider only the parameter of energy produced, we would get a final arrangement with high productivity but with poor economic optimisation, which we would get if we were to evaluate the parameter of the level of energy costs. On the other hand, if we were to consider only the latter, we would get an extremely expensive arrangement, probably amortised by the economies of scale, but ignoring the importance of the initial investment.
Having established these necessary premises, we can move forward in the analysis of the process and conclude how much the parameter of the levelised cost of energy taking into account both the producibility according to the disposition of the turbines, and its cost. Therefore, in the first instance, it will be the most important parameter we will analyse.

The code will consist of functions belonging mainly to two libraries. The first will deal with the implementation part of the genetic optimisation (purple in the scheme), the second will simulate the aerodynamic field of the individual (green in the scheme) and return the parameters of the performance we are interested in. These two libraries need to be paired in order to work synergistically.
The coupling of the two libraries is the most complex part of the work, as they are articulated and heavy algorithms that have to be tuned to each other by changing parameters and structures.
The final version of the algorithm obtained is shown in the diagram below and sees as primary algorithm that of genetic optimisation, using the library called Pymoo, with the creation of the random arrangements of the arrays and their composition in generations. After that, it will be this algorithm to launch the next, individual by individual, based on the PyWake library, to evaluate the performance and thus the annual energy production of the array.

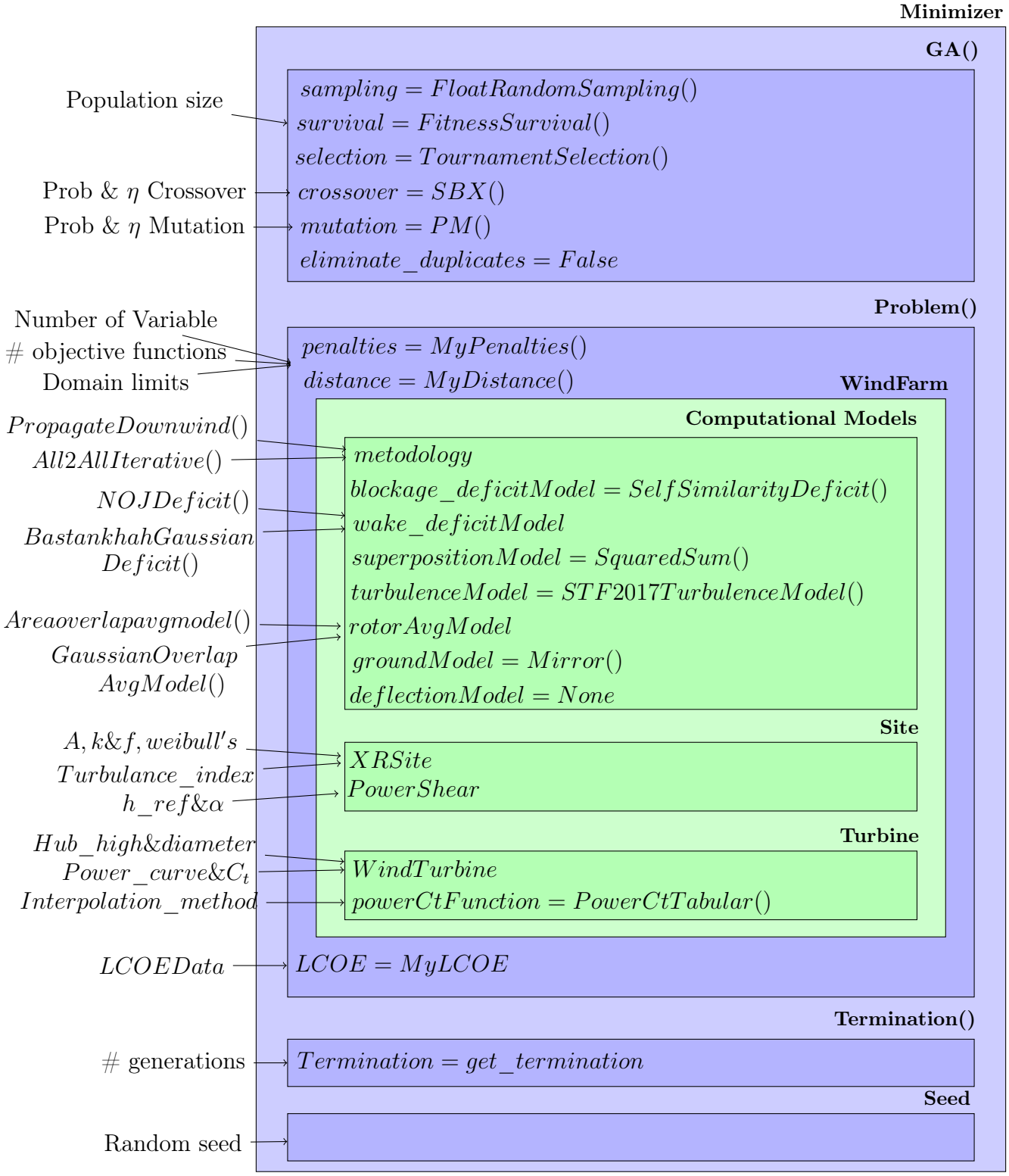

In this diagram, you can see the models selected for the simulation characterized by the brackets: *()*, Python style. They are assigned directly to the class concerned with an equal sign if unique, or with an arrow from the left if they present alternatives. Moreover, summarised on the left are the inputs for the simulation.

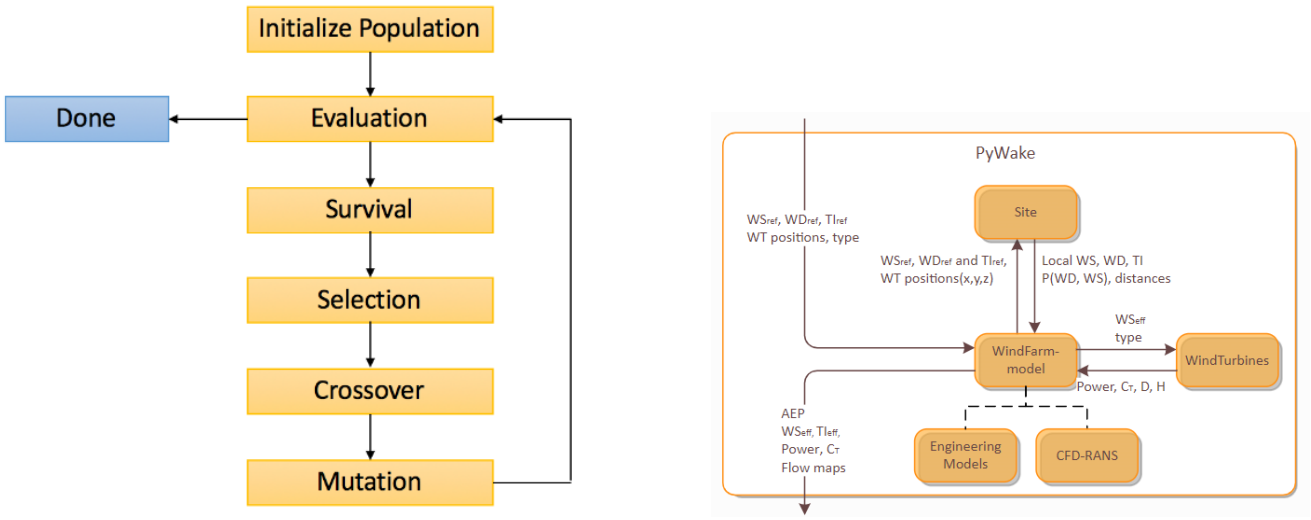

(a) Genetic algorithm in Pymoo (b) Flow field simulation in PyWake

Figure 3: Pymoo and PyWake flowcharts

The following discussion will be divided into three chapters: the first two that correspond to the main parts of the algorithm, the **implementation of the genetic algorithm, Pymoo library** and the **implementation of the aerodynamic analysis and the wind farm productivity, PyWake library**. The third chapter, technically less crucial than the previous ones on the **implementation of the LCOE, calculation and hypothesis**, still requires a widely in-depth treatment.

4.1 Implementation of the genetic algorithm, Pymoo library

As discussed erlier, it exist several different type of optimization algorithm family and type. However, as we have seen, we have been able to condense into a single parameter, the *LCOE*, various aspects of the analysis, such as productivity and compactness, as discordant as they are. Consequently,

Based on the contingent characteristics of the problem under discussion in this thesis; considering the size of the search space and its structure (with constraints and local minima), and taking into account the choice of optimizing the different requests of the problem condensed in the parameter of *LCOE*, we discarded the optimization through *NSGAii* and opted for an optimization through genetic algorithm. A robust and flexible algorithm capable of finding global solutions or close to the global in complex problems and in a parallelizable way.

As already introduced, for the implementation of the genetic algorithm we have selected the Pymoo library that is an extremely comprehensive and structured library that offers the possibility to optimise according to many types of algorithms.
From this we have selected the functions that allow the optimisation of the genetic type for single objective problems; this is, in primis, the function GA. This function in turn depends on numerous parameters that provide the possibility to manage and adapt the optimisation based on the contingencies required for the problem. Starting with the number of free variables and their constraints, and ending with the parameters that determine the shape of the probability distribution function of the mutations that affect the generation of the next generation.

To perform the minimization is selected the Pymoo function *minimize* as shown in the diagram above.
To correctly use it is necessary to define: the **algorithm** with which minimisation is to be performed, the **problem** to be minimised, the **termination parameter** and the **seed** that determines the random evolution of the simulation.

4.1.1 Genetic Algorithm

besides, defining the GA function are required several parameters such as the size of the population of each generation, **pop_size**, what kind of **sampling** to perform or what kind of **survival** strategy and and with **selection** method. And furthermore the **crossover** and **mutation** parameters for the shape of their probabilistic functions. These choices are crucial, as they determine the progress of the optimization.

- **Pop_size**; Population size is a crucial parameter for the correct implementation of optimisation. Indeed, a too-small population within the generation would not guarantee the necessary diversification to achieve all possible dispositions. For example, if the objective function has a peak that records a collapse with minimal variations in the value of the free variable and therefore requires a large number of simulations to be found by the mutations because it is difficult to achieve with the simple course of optimisation.

- **Sampling**; determines how the first generation of individuals is generated.
  These are methods that allow to generate initial points for the genetic algorithm. The difference between the various types of sampling depends on the type of variables you want to generate or on the distribution of points in the space of solutions.
  For example, Pymoo's library function *FloatRandomSampling* produces random points in the range of real variables, while *BinaryRandomSampling* generates random points in the range of binary variables. Other sampling methods try to distribute points more evenly in the solution space, such as *LatinHypercubeSampling*, which divides the space into cells and assigns a point to each of them. This can be useful to better explore the solution space and reduce the correlation between points.[52]

  For all the simulations presented below, the FloatRandomSampling method will be used.

- **Survival**; determines the survival strategy, which establishes which solutions are retained or discarded after a generation.
  In the calculations, we will use the class FitnessSurvival, which selects the solutions with the best fitness according to the criterion of the local minimum, where fitness is the value of the objective function to be minimised.
  The function follows the logic of checking for each individual which one complies with the boundary conditions and which one does not. If both do not comply with the constraints, the function "Compare" is used to select the solution with the lower value of boundary condition violation. If the two solutions have the same constrain violation value, the function selects a random solution. If both solutions are feasible (i.e. they have a value of zero for constraint violation), then the Compare function is used to choose the solution with the best fitness value. If the two solutions have the same value as fitness, then a random solution is selected. [50].

- **Selection**; is a class that defines the parent selection method for the crossover.
  There are various selection strategies that can influence selective pressure and population diversity. *RandomSelection*, for example, randomly chooses parents from the current population, while *TournamentSelection* chooses parents through competition between a fixed number of individuals. Selection can be based on various criteria, such as the value of the objective function, the degree of feasibility or the distance to other individuals. [53] For subsequent calculations, the *TournamentSelection* method implemented by default is chosen and the fixed number of individuals are those who do not violate constraints.

- **Crossover**; The crossover operation is an operation that consists in combining two or more existing solutions (called parents) to generate one or more new solutions (called children). Crossover makes it possible, to create solutions that inherit the best characteristics of the parents and to increase genetic diversity in the population.
  Crossover is inspired by the recombination mechanism that occurs in sexual reproduction in biology. is a fundamental operation in genetic algorithms, which are heuristic methods for solving complex optimisation problems.

  For calculations that work with real variables for which the binary crossover is not applicable, the class *SBX (Simulated Binary Crossover)* is therefore used. This method produces values that are similar to those of the parents and have a symmetrical distribution around the average of the parents.

  You can define the parameters prob and η of the probability distribution.[54] If the crossover probability is high, it means that two parents are more likely to mate to have children, combining their own qualities. If the crossover probability is low, it means that the children are more likely to be equal to the parents.

  On the other hand, if the value of η is low, the distribution is wider and the children may have quite different values from their parents. This encourages the exploration of the research space and diversity in the population. Conversely, when the value of η is high, the distribution is narrower and the children have very similar values to their parents. This promotes the exploitation of the best solutions and convergence towards a minimum.

  The choice of the optimal values of these last two quantities is not trivial, because it is necessary to find the compromise between exploration and deepening. Some methods even consider values that are not constant during the simulation.

  In the calculations presented below the GA default values will be used.[55]

- **Mutation**; the mutation operator randomly modifies a solution to introduce diversity into the population. In the calculations, the PM (Polynomial Mutation) class is used, which uses a polynomial distribution to produce values that are close to the original value.

  Mutations are also inspired by events of sexual reproduction in biology. They are also a fundamental operation in genetic algorithms because they allow to introduce further diversity in the population and to avoid that the algorithm gets stuck in a local minimum, and together with crossover operations they are the reason for the name of this optimization technique.

As for the crossover, it is possible to specify the prob and η parameters of the probability distribution. And as for the crossover, parameter η determines the differentiation of mutations leading to individuals being very or slightly different depending on whether it is high or low in value. Whereas the probability parameter indicates how likely it is that a mutation occurs or not.

- **Eliminate duplicate**; allows to eliminate duplicate individuals from the generation. This ensures greater diversification and thus better convergence. However, in the simulation under examination, the individuals are composed of several tens of real variables. This makes it extremely unlikely that two individuals can be exactly the same. For this reason and to reduce the calculation times, we choose not to verify that there are no duplicates by setting *Eliminate_Duplicate* to *False*.

4.1.2 Problem

Continuing with the definition of the minimization function, is necessary to define also the problem to minimize. This is the most complex part of the algorithm; indeed it is the link between the optimization the aerodynamic simulation algorithms.

This is where the number of free variables, **n_var**, is defined; i.e., the x and y positions of the turbines in the array (and consequently the number of turbines) and the number of parameters to be optimized, **n_obj**; namely the objective of the analysis. Or the number of constraints to be considered, **n_ineq**. Moreover, it is in the problem definition that the boundary conditions, **BC**, must be inserted. These are the limits of the domain within which the free variables x and y can vary. And, above all, it is in the problem definition where the functions created ad hoc for this work are used to evaluate: **penalties**, **distance** and **lcoe**. And, in the end, the performance of **windfarm**, through the PyWake library's functions.

- **n_var**; the number of free variables is crucial as it determines the number of turbines within the array. All the subsequent considerations depend on this since a very dense arrangement could allow for a better scale economy; however, it would also imply a worsening in the productivity of the individual turbines due to the shadow effect that they exert on each other.

  In some types of analysis presented later, the value of n_var will consider not only the number of x and y variables of the turbine positions, but also a boolean variable for each of them to determine their model.

- **n_obj**; come trattato in precedenza, sarebbe stato possibile eseguire l'analisi in modo multi-obbiettivo, ma si è optato per consendare i diversi aspetti del problema nel parametro dell'$LCOE$. Cosi facendo il numero di obbiettivi sarà uno perchiò: $n\_obj = 1$.

- **n_ineq**; indicates the number of inequality constraints of the problem. In the simulations under examination there are none of these constraints.

- **BC**; determine the limits of the domain, which is one of the main parameters of the problem. Together with n_var it defines the density of turbines, and therefore, as a consequence, all the values of the performance of the array.

As mentioned for n_var, the BC, in some analyses will contain not only the upper and lower limits of the x and y variables but also the two states of the boolean variable that determines the type of turbine to be inserted in the array.

- **Penalties**; consist of performing checks that, if failed, result in a penalty that within the genetic optimization determines a lower probability of reproducing the penalized individual in subsequent generations.[56]

  Specifically in our case, we impose that each turbine has a free zone around it where no other turbines can be present. That is, any configuration that sees the overlap of the minimum distance dedicated to a turbine, with that of another, is penalized.

  In practice, a circumference of 1.5 times the diameter is considered around each turbine. For each them, the distance from all the turbine is calculated and in case of overlap, the intensity is calculated, so as to attribute to this overlap a penalty commensurate with its severity. This last precaution is adopted to facilitate the algorithm by indicating the direction of resolution of the overlap.

  In order to speed up the calculation time, the aerodynamic performance evaluation is performed only for the individuals without penalties. This means that the verification of the boundary conditions occurs in the genetic algorithm, after the definition of the individual's coordinates, but before the aerodynamic analysis.

  The step of inserting penalties was necessary in order to obtain non-trivial solutions. In fact, in the absence of penalties, often, a collapse of the coordinates of several turbines was observed. That is, to avoid the shadowing effect in the wake, the genetic algorithm determined as the best arrangement a configuration with all the turbines overlapping each other.
  This is obviously physically unacceptable and the adoption of penalties perfectly solves the problem.

  Moreover, the introduction of penalties allows to follow the rule of thumb guidelines that indicate the distance of 3/5 times the diameter between one turbine and another, as the approximately ideal distance to facilitate the aerodynamic efficiency and the compaction of the array. In fact, as it is constructed, the structure of penalties guarantees a spacing between turbines of 3 times the diameter.

  In some particular simulations that will be discussed later, it was chosen to apply also an additional type of penalty.
  In fact, in some simulations the type of turbine is not constant for all the wind generators in the wind farm but, rather, it is free to change between two possible models depending on the evolution of the genetic algorithm.
  It was preferred not to leave the algorithm completely free to determine the model of each element, but to manage the limits within which the algorithm could move through penalties. This means that for simulations with mixed turbine models, the presence of at least 1/3 of turbines per type will be guaranteed.

- **Distance**; The distance between the turbines is an important parameter in the evaluation of the $LCOE$.

This analysis can be carried out according to various hypotheses. Specifically, the most accurate solution is called the "Travelling Salesman Problem" and it is of particular importance in terms of computational calculation because it is an exponential problem without a polynomial solution.[57] This calculation can be simplified by using approximate algorithms, which provide an estimate of the result by introducing an error.[58] However, in our solution, we used the hypothesis that the electric transformation station, where the transformers that have the task of increasing the voltage from medium to high are contained, is located at the midpoint of the x and y coordinates of all the wind turbines. And, moreover, each wind generator is connected independently; that is, that the length of the medium voltage cables is the sum of the distances of each turbine with the electric transformation station.

- **WindFarm**; the discussion of the algorithm part that simulates the wind farm velocity field is deepened in section 4.2.
- **LCOE**; The treatment of the algorithm part for the $LCOE$ calculation is deepened in section 4.3.

4.1.3 Termination

The termination parameter can be of various types, such as a time parameter, a limit of the number of simulations, of generations or a tolerance parameter with respect to the variation of the purpose of the analysis. In all our analyses, for a matter of repeatability of the experiments we will use the number of generations as a parameter beyond which to stop the simulation through the function *get_termination*

4.1.4 Seed

The seed must be a random parameter to determine the validity of the results. Nevertheless, most of the preparatory simulations were performed with a fixed seed to allow the direct comparison of the results and quickly evaluate the effect of the changes made. Afterwards, the results obtained later are all fruits of simulations with random seeds.

4.2 Implementation of the aerodynamic analysis and the wind farm productivity, PyWake library

PyWake is a Python library that allows one to perform wind farm simulations with different levels of complexity and flexibility. The library allows us to set up the wind speed conditions, the solar irradiation data, the characteristics of the turbines and the wake propagation models.
Moreover, it offers a wide range of models to be able to specify in detail the type of analysis to be performed. Starting from the simulation of a site based on constant wind speed data, arriving to productivity analyses of sites based on data from *Pvgis*. It allows one to customize turbines and use a calculation model of upwind or downwind propagation, whether or not to consider an overlapping area model, a wake deficit model and a tilt adjustment.

In the aerodynamic simulation model used in this thesis, we consider three macro classes that we will define in detail: the **calculation models** implemented, the **site** of interest and the **turbine models** used.

4.2.1 Calculation models

For the analyses of this thesis, two different calculation models are defined. The first one favours performance in terms of calculation times, and the second one allows to obtain more accurate results.
One model or the other will be used depending on the needs of the analysis.

The main difference between the two calculation models is the procedure with which the analysis are performed. It can take place in the direction favourable to the wind current or in an iterative way; that is, according to the methods called respectively *PropagatedDownwind* and *All2AllIterative* and further developed below.

Moreover, the calculation models will be composed by the joint use of other models for the simulation of:

- **Blockage_deficitModel**, which calculates the blockage effect, that is the perturbation of the wind field caused upstream by the turbine itself. [43]
- **WakedeficitModel**, models the reduction of wind speed caused by a wind turbine that extracts energy from the airflow by defining the propagation of the wake downstream. [43]
- **SuperpositionModel**, calculates the effective wind speed given the local wind speed and the deficits calculated by the other models. [43]
- **TurbulenceModel**, calculates the increase of turbulence intensity in the airflow, due to the presence and effect of the turbine. [43]
- **RotorAvgModel**, defines one or more points on the turbine rotor to calculate the average wind speed incident on it. [43]
- **Groundmodel**, models the effects that the ground has on the flow entering the turbine and on the wake. [43]
- **DeflectionModel**, calculate the deflection of the wake due to yaw misalignment or shear flows. [43]

The simplest of the two calculation models will implement the *PropagatedDownwind* methodology and will consist of the *NOJDeficit* wake deficit model and the *SquaredSum* effects overlap model. I did not add the default models: for turbulence management, wind deflection and soil behaviour. While to model the rotor I use the *AreaOverlapAvgModel*, as shown in the algorithm diagram in section 4. And this, as a fair compromise between performance and computation time. On the contrary, the most accurate model will implement the *All2Alternatives* methodology and will use the *SelfSimilarityDeficit* block deficit model. It will consist of the *BastankhahGaussianDeficit* wake deficit model and the same effects overlap model; *SquaredSum*. However, I add the *STF2017TurbulenceModel* turbulence management model and the *Mirror* class to model the soil. Moreover, as a rotor modeller I use the *GaussianOverlapAvgModel*, while, as before, I do not define any model for managing deflections.

- The fastest methodology is *PropagatedDownwind* which is preferred over the alternative *All2Alternatives*, although it introduces some approximations, depending on the type of

calculation that is performed.
The main difference between the two is that the first one performs the minimum possible number of deficit calculations proceeding in the direction of the airflow. Starting from the first turbines with respect to the airflow and applying on them the models to simulate the effects presented above. Then it moves on to the next turbines considering an airflow modified by the effect of the previous turbines.
Figure fig. 4a shows the procedure where: at "*Iteration 1*: $WT0$ sees the free wind (10 m/s). Its deficit on $WT1$ and $WT2$ is calculated."[43] And, continuing with the description, at "*Iteration 2*: $WT1$ sees the free wind minus the deficit from $WT0$. Its deficit on $WT2$ is calculated and the effective wind speed at $WT2$ is updated."[43]

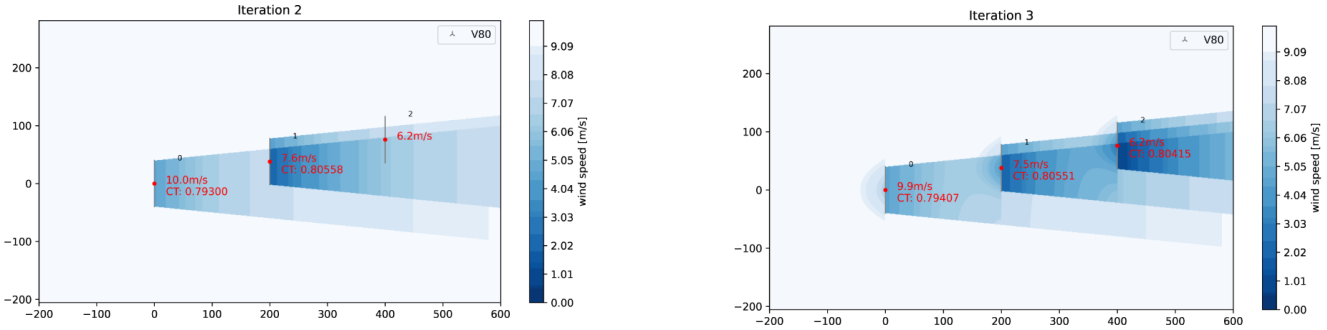

(a) PropagateDownwind (b) All2AllIterative

Figure 4: Illustrations of different processes

On the other hand, the second procedure iterates over all turbines in order from downstream to upstream until the result exceeds a tolerance threshold. This is because it also takes into account the blockage effect, which the previous procedure neglected. Namely, *All2AllIterative* also considers the fact that the presence of a downstream turbine can influence the wind incident on an upstream turbine.
The only way to consider this effect is to proceed iteratively. Therefore, at each iteration, the effective wind speed at the examined turbine is calculated, as free wind speed minus the sum of the deficit from the upstream sources. Based on this effective wind speed, the deficit caused by the current turbine on all downstream destinations is calculated. This second methodology, introducing the iterative calculation on all turbines in the park, greatly increases the calculation times.
With reference to fig. 4b the procedure it is:

- "*Iteration 1*: All three WT see the free wind (10 m/s) and their CT values and resulting deficits are therefore equal.
- *Iteration 2*: The local effective wind speeds are updated taking into account the wake and blockage effects of the other WT. Based on these wind speeds the CT and deficits are recalculated.
- *Iteration 3*: Repeat after which the flow field has converged."

[43]

- **The blockage effect** derives from the conservation of momentum that is reduced by the presence of the turbine, and sees part of the reduction also reflected upstream.
  It consists of the decrease in the speed of the air column upstream (as well as the more obvious reduction in wind speed downstream), due to an obstacle. This means that the producibility of a turbine not obstructed by others must still be recalculated iteratively based on what happens behind it.

  In the first calculation model, I do not use any *blockage_ deficitModel*, as *PropagatedDownwind* does not consider this effect in order to favour the calculation times.
  Instead, in the second calculation model I use for greater accuracy the *SelfSimilarityDeficit*. This model simulates the induction zone of wind turbines through the analytical formula(4), assuming that the induced velocity is independent and self-similar. Therefore, assuming that the spatial distribution of the induced velocity, and therefore the wake, has the same shape and properties (density, pressure, temperature and velocity), regardless of the distance from the rotor and its size, or the shape, number and arrangement of the blades.
  In other words, this means that a wake with universal and predictable behavior is assumed.[59], [43].

$$v_{\text{eff}} = v_\infty \left(1 - \frac{1}{2}\left(1 - \sqrt{1 - C_T}\right) \operatorname{sech}^\alpha(\beta\epsilon)\right) \tag{4}$$

  - v_{eff}: is the effective wind speed at a certain distance from the wind turbine, measured in meters per second $[m/s]$. It is the one that is observed taking into account the presence of the wake.
  - v_∞: is the free wind speed.
  - C_T: is the thrust coefficient of the wind turbine, a dimensionless quantity that measures the fraction of kinetic energy of the wind that is extracted by the turbine. It varies between 0 and 1, where 0 means that the turbine does not extract any energy from the wind and 1 means that the turbine extracts all the energy from the wind (ideal but unrealistic situation). The thrust coefficient depends on the type of turbine, its design and operating conditions. [59]
  - α and β: are parameters that depend on the local Reynolds number.
  - ϵ: is the normalized distance from the center of the wake, that is, the ratio between the distance from the center of the wake and the radius of the wake itself. This quantity characterizes the shape of the wake according to the assumption of self-similarity. [59]

- As a **wake deficit model** I use the NOJDeficit for the lighter model and the BastankhahGaussianDeficit for the more accurate model.

  The first one involves the implementation of the analytical Jensen model presented in section 3.1.5. A simple and fast model for simulating the aerodynamic wake that assumes that the wake expands linearly with a constant k that depends on the turbulence intensity.
  The second one, instead, presented in section 3.1.6, calculates the wind speed deficit based on an analytical formula based on the assumption of a Gaussian distribution of the wind speed in the wake.

Therefore, both use analytical formulas to calculate the wind speed deficit.
The *NOJDeficit* is based on eq. (2) with the assumption of a top-hat distribution of the wind speed in the wake and uses a constant expansion parameter.
On the contrary, the *BastankhahGaussianDeficit* is based on eq. (3) with the assumption of a Gaussian distribution of the wind speed in the wake and considers different factors that influence its shape and expansion.
The latter is more accurate but also more complex than the *NOJDeficit*. The former is simpler but also more conservative than the *BastankhahGaussianDeficit*.
This greater conservatism is necessary to avoid underestimating the wake effect. As a consequence, using the calculation model less demanding in terms of computational time, one tends to obtain a more severe wake effect.

The choice of these models and the consequent exclusion of all the others discussed in section 3.1 is due to computational costs. In fact, by integrating them with a genetic optimization algorithm, their use becomes intensive and incompatible with the implementation of *CFD* calculations.
The two are further discriminated in terms of computational commitments by using the *NOJDeficit* for the faster calculation model, to be used for the most time-consuming optimizations. Conversely, *BastankhahGaussianDeficit* will be used for simulations where greater accuracy is required.

- As **Superposition model**, instead, I set the *SquaredSum* for both calculation models.
  This is a model that calculates the effective wind speed given the local speed and the deficits (typically from multiple sources). Therefore it uses and overlaps the results obtained by applying the *WakedeficitModel* creating the final wind speed field.
  The *SquaredSum* model uses the following formula for the sum of the deficits [60]:

$$u_{eff} = u_{loc} - \sqrt{\sum_i \Delta u_i^2} \tag{5}$$

  Where u_{eff} is the effective velocity, u_{loc} is the local velocity and Δu_i are the deficits caused by the different sources of wake perturbation.
  The model assumes that the deficits add up as the square root of the sum of squares, which implies that the total deficit cannot be greater than the local velocity.

  The alternative could have been the *LinearSum* model, which calculates the effective wind speed as the linear sum of the deficits. However, this choice was not made because it is less accurate.[43]

- The **turbulence models** describe how the wind turbine reduces the wind speed and increases the turbulence in the wake. This has an impact on the downstream turbines, which receive a more turbulent wind. Each model uses a different formula to calculate the velocity deficit and the turbulence in the wake as a function of the distance from the turbine, the thrust coefficient, the free wind speed and other parameters. Many of them are based on empirical formulas such as those of Crespo and Herna'ndez or Gunner Chr. Larsen.[61], [62]

In the fastest calculation model I decided to neglect this effect as well, always to safeguard the calculation times.
I did not do the same for the more complex model where I also consider the effects of turbulence using the STF2017TurbulenceModel class. Namely, the "model of Steen Frandsen implemented according to IEC61400-1, 2017"[43].
The turbulence intensity is calculated based on this formula:

$$TI_{out}^{ijlk} = w^{ijlk} \left(\sqrt{\left(\frac{1}{c_0 + c_1 \frac{d^{ijlk}}{\sqrt{C_T^i}}} \right)^2 + (TI_i^{lk})^2} - TI_i^{lk} \right) \tag{6}$$

Where:

- TI_{out}^{ijlk}; contains the turbulence intensity at the wake exit for each pair of turbines, level and wind direction.
- w^{ijlk}; are the weights, for each pair of turbines depend on level and wind direction and on the angle between the wind direction and the line that connects the turbines.
- d^{ijlk}; is the normalized distance between the turbines.
- C_T^i; is the thrust coefficient.
- c_0 e c_1; are empirical constants that depend on the type of turbine and the site.

[63] The formula calculates the turbulence intensity at the exit of the wake of a wind turbine as a function of the ambient turbulence, the amplification factor of the turbulence induced by the wake, the distance and the angle between the turbines, the thrust coefficient and empirical parameters specific for the type of turbine and the site.[63]
The turbulence intensity will then be used as additional data to calculate the wake deficit more accurately.

- The **Rotor Average Model** simulate the rotor evaluating the wind speed on it and combining the data with the information on the wake, generated by the previous turbines.

  There are several models to perform this calculation. And their choice also depends on the wake deficit model type.
  The simplest and applicable to any wake deficit model is the *RotorCenter* that uses only the speed at the center of the rotor as information. In fact, it is fast from a computational point of view but introduces considerable approximations, not even considering the relative position of the rotor with respect to the calculated wakes.[43]

  The most suitable model for the wake deficit model based on the analytical formulas of Jensen, *NOJDeficit*, is the *AreaOverlapModel* which we will use in the first and fastest calculation model. It is a rotor approximation model that calculates the overlap factor between the rotor and the wake of another wind turbine based on the common area between the two disks. This model is used to reduce the effect of grid discretization calculated with the Jensen model, and only makes sense coupled with it because they both use cylindrical geometries, the latter defining a cylindrical wake.

"The calculation formula can be found in the first equation in [64]",[43].

The *GaussianOverlapAvgModel* is the most suitable to use in combination with *Bastankhah-GaussianDeficit* as they both work with Gaussian probability distributions for the speed.[43] The intensity of the disturbance caused by a previous turbine on a subsequent one (with respect to the wind direction), depends on the extent of the overlap of the wake produced by the first with the rotor of the second. To take this into account, we use formula (7):

$$\delta_{i,j} = \frac{1}{A_j} \int_{A_j} \frac{\Delta u_{i,j}}{u_{0,j}} dA = \frac{C_j(x_{i,j})}{A_j} \int_{A_j} \exp\left(-\frac{r^2}{2\sigma^2_{w,i}(x_{i,j})}\right) dA \tag{7}$$

[65],[43].

(7) calculates the average of the wake of turbine j that overlaps the disk of rotor i.
Dove:

- $\delta_{i,j}$; is the average velocity deficit.
- A_j: is the area of the downstream rotor.
- $\Delta u_{i,j}$; is the local speed deficit caused by the wake of the upstream wind generator.
- $u_{0,j}$; is the free wind speed on the downstream wind generator.
- $C_j(x_{i,j})$: is the thrust coefficient of the upstream wind generator, which depends on the distance between the two wind generators.
- $\sigma_{w,i}(x_{i,j})$; is the characteristic width of the upstream wind generator's wake, which depends on the distance between the two wind generators and the expansion parameter of the wake.
- r; is the radial distance between the centre of the trail and the point considered on the surface of the downstream rotor.[65]

- To model the **ground** in the fastest calculation model I chose to use the default model that ignores the effects of the ground, as the surface in the open sea is the simplest to consider and a light model reduces the calculation time without introducing a noticeable error.
  I chose, instead, to use the simplest alternative for the most accurate calculation model. It is a model called "Mirror" and it "Consider the ground as a mirror (modelled by adding underground wind turbines). The deficits caused by the above- and below-ground turbines are summed by the *superpositionModel* of the *windFarmModel* ".[66]

- The **deflection models** are used to describe how the wake produced by a wind turbine is deflected by the crosswind and the yaw misalignment, both in the lateral and vertical directions. This deflection affects the position and shape of the wake downstream of the turbine and its impact on the adjacent turbines.

  This phenomenon of the wind is not considered in our calculations because it significantly increases their complexity while providing a negligible contribution, also and especially because the resource in the site under analysis is markedly directional and, therefore, the amount of crosswind is minimal. [43]

4.2.2 Site

The site considered in the analysis belongs to an area off the island of Pantelleria.
The historical data on the wind availability were provided by the research group of the Polytechnic of Turin, More.

The database consisted of 87600 measurements of wind speed and direction; that is, the equivalent of one measurement per day for 10 *years*.

On PyWake, the site can be defined in the most general way possible by specifying all the necessary characteristics.
In the thesis, it was chosen to define the availability of the wind resource in a very precise way, namely, through a **Weibull** curve for each sector considered.
The raw data of wind speed and directions, measured every hour, were first of all divided into 24 sectors. Then, they have been averaged to obtain a value representing the annual average for each direction.
From this data processing, the availability of the resource is shown in fig. 5.

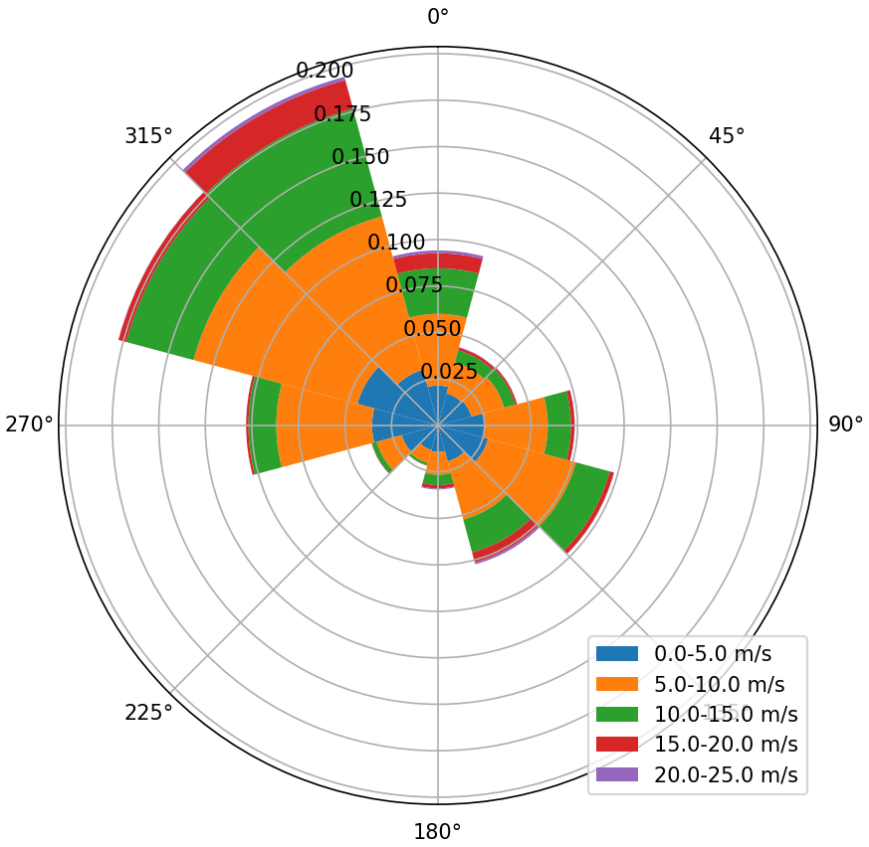

Figure 5: Wind rose in Pantelleria

From it, it can be seen how the wind is particularly directed, to be precise towards the southeast, from the northwest. This characteristic will greatly influence the arrangement of the generators which will tend to arrange themselves in such a way as to favor it.

The most general class of PyWake that allows one to completely customize the site is *XRSite*. It will be provided with the values of scaling parameter, A and shape of the *Weibull* curve, k, for

24 times as many as the sectors of subdivision of the angle turn together with the frequencies f of the sectors.
The evaluation of the A and k parameters is done by the **Matlab** function *fitdist*. To these data, I also add the value of the turbulence parameter, constant and equal to 0.1.
Based on the value of the speed at a specific height, it is possible to extrapolate the speeds to the other heights; therefore, lastly, I provide *XRSite* with the function for extrapolation.

Considering that the value indicated by the **Weibull** curve is a probabilistic value, for a specific height above sea level, the information in the database is not sufficient to satisfactorily simulate a real speed field. Thanks to analytical relationships such as the logarithmic law or the power law, I can extend the information in height.
However, considering that the first one is particularly suitable for heights below 100 m, in the calculations it was decided to set the extrapolation based on the second one, which uses equation 8.

$$u = u_r \left(\frac{z}{z_r} \right)^{\alpha} \tag{8}$$

Where:

- u; is the extrapolated wind speed.
- z; is the height at which you want to evaluate the speed.
- u_r; is the known wind speed at a reference height, z_r.
- α; is an empirical coefficient that varies according to the stability of the atmosphere. For open sea conditions, as in the present situation, it has a value of 0.11.

PyWake implements this function through the *PowerShear* method, in which the reference height and the coefficient α must be specified. In this case we set $z_r = 10m$ and $\alpha = 0.11$
By doing so, albeit at the expense of computational times, the simulation is also distributed in height, for values that would otherwise have been excluded. This allows to consider also turbines of different heights. Indeed, in some analyses presented later, the turbine model will be a free variable and this expedient will allow to obtain sensible results.

Finally, in the *LCOE* calculations that will be discussed later, we will consider a seabed depth of $180m$.

4.2.3 Turbine models

The PyWake library allows you to define the characteristics of the turbines to simulate.
These qualities influence the turbine's ability to extract energy from the airflow, thus the power production of the individual turbines, but also determine the disturbances of the flow field, and therefore, ultimately, also the annual energy production of the wind farm itself.

The main parameters that determine the performance of a turbine are the hub height, the rotor diameter, the power curve and the thrust factor curve.
The power curve represents the electrical power that a turbine can produce from the available

wind resource. It is a fundamental property to evaluate the performance and producibility of a turbine in a given site.
The thrust coefficient is a parameter that describes the force that the wind exerts on the wind turbine, and therefore its ability to extract kinetic energy and translate it into rotational motion. "It is calculated as the ratio between the force exerted on the actuator disk and the force available in the wind"[67].

In the implemented calculations, we chose to use two different models of turbines that we will call *Small* and *Big* and that correspond to the models: *NREL_5MW_126_RWT* and *LEANWIND_8MW_164_RWT*.
The data comes from the database in [68].

We also chose that all the turbines are floating of the *Spar-buoy* type with a three-cable mooring system and a gravitational anchoring system. Definitions that will be useful for the economic calculations performed in the *LCOE*.
They vary, instead, for the two models the values of nominal power, hub height and rotor diameter, as shown in table 1. They also vary the power curves and those of the thrust coefficient and, with them, the *cut-in* and *cut-out* speeds, and this is appreciable from the graphs in fig. 6, fig. 7, fig. 8.

Table 1: Wind turbines parameters

	Wt *Small*	Wt *Big*
Nominal Power [MW]	5	8
Hub high [m]	90	110
Rotor Diamiter [m]	126	164

As for the power curve, it depends on several factors, both physical and technological, and among the most relevant there are the constructive characteristics of the turbine, such as the diameter, the hub height, the type of generator, the control system and the thrust coefficient itself.

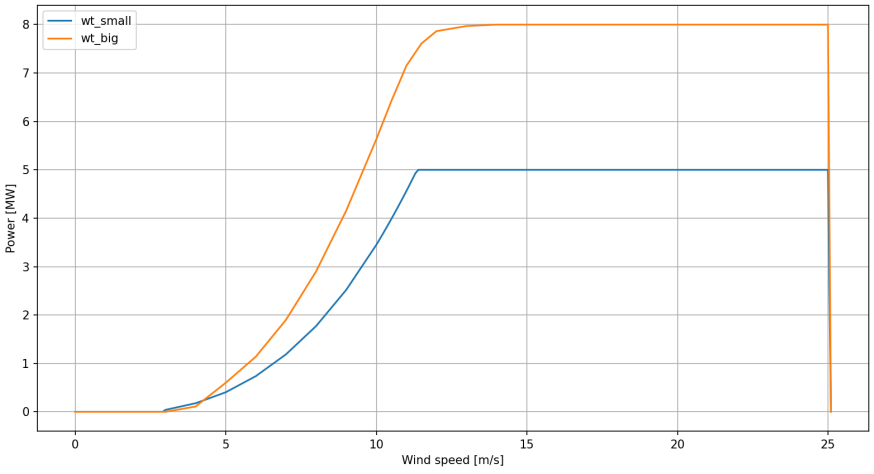

Figure 6: Power curves

These factors determine the shape and the maximum value of the power curve. The diameter

of the turbine determines the swept area and therefore, the amount of wind intercepted by the turbine. The hub height determines the height at which the turbine is exposed to the wind and therefore its quality. The type of generator determines how the mechanical power is converted into electrical power. The control system determines how the turbine adapts to the variations of the wind and the operating conditions. While it is the thrust coefficient that determines the aerodynamic effects.[69], [67]

As can be seen from fig. 6 the power curve has a shape characterized by four main regions:

- The first one, before the *cut-in* velocity where the wind speed is too low to rotate the turbine and the power produced is null or negligible.
- The second one, the start-up region. It is after the *cut-in* velocity where, depending on the control strategy, the power produced grows with the third power of the wind speed, until reaching the maximum nominal value of the turbine.
- The third, the nominal operating region, where the power produced reach the maximum nominal value of and remains constant independently of the wind speed until reaching the *cut-off* velocity of the turbine.
- The *cut-out* region, where the wind speed exceeds the critical or shutdown value and the control system switch down the turbine. Therefore the power produced is null to protect the turbine from structural damage.

[69] As can be seen from fig. 6, we would expect a much higher producibility for the *Big* turbines. This is due to the simple value of nominal power that the different models reach before the *cur-off* speed.

As for the thrust coefficient, it indicates how well the wind turbine transforms the kinetic energy of the wind into the mechanical energy of the rotor, according to the equation. Moreover, it allows to evaluate the resistance that the wind turbine must oppose to the wind and therefore the robustness of its structure: $C_t = 4a(1-a)$, where a is the induction factor.
A too-low thrust coefficient means that the wind turbine exploits to a small extent the wind, while a too-high thrust coefficient means that the wind turbine slows down too much the wind and therefore reduces its efficiency.
The thrust coefficient is influenced by the pitch angle, the yaw and the tip speed ratio.
The pitch angle is the angle between the rotor plane and the blade plane. This angle determines the angle of attack of the wind on the blade and therefore the thrust and power coefficient of the turbine. The yaw is the angle between the rotor axis and the wind direction. This angle determines the alignment of the turbine with the wind and therefore the amount of power that the turbine can extract from the wind. The tip speed ratio is the ratio between the tangential speed of the tip of the blade and the wind speed. This ratio determines the aerodynamic performance of the turbine and therefore its efficiency.
In conclusion, it can be said that the thrust coefficient curve summarizes the efficiency of the generator, the conversion system and the aerodynamic performance of the blades.[69], [67]

As can be seen from the graph, the turbines behave very differently at the same wind speed. This allows for a greater variety and allows the algorithm to select the most appropriate one for the site of interest.

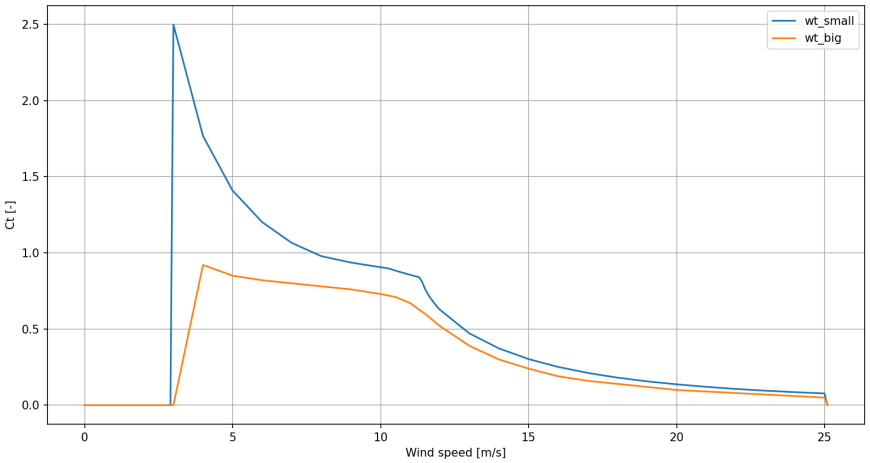

Figure 7: Thrust Coefficient Curves

A particular value to analyze is that of the thrust coefficient of the turbine model *Small* for lower speeds. Indeed, we see a Ct greater than one. This is strange because it means that the rotational energy of the blades is greater than the kinetic energy of the incident wind. One possible explanation is that the turbine is designed with a high aspect ratio, meaning that the blades are longer and narrower than usual. This design allows the turbine to extract more energy from the wind but also increases the amount of drag that it experiences.

Another parameter indicative of the performance of a turbine is the power coefficient C_p shown in fig. 8.
The curves show how the efficiency of a wind turbine varies as a function of wind speed according

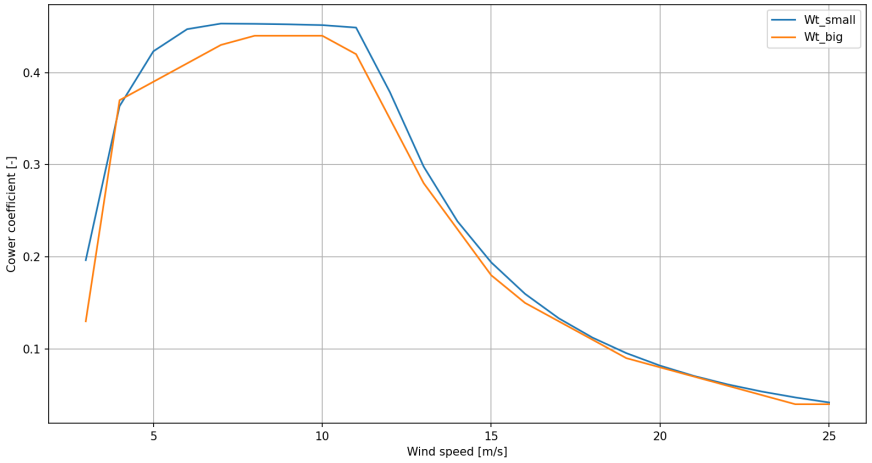

Figure 8: Power Coefficient curves

to the equation $C_p = 4a(1-a)^2$.
It is also possible to check how all curves comply with Beltz's theoretical maximum limit of 0.593.[70]

The implementation of the *turbine* class on PyWake is done by providing the *WindTurbine* class with the values discussed so far of hub high and rotor diameter. While the values of the Power curve, Thrust coefficient, are provided using the *PowerCtTabular* function.

The role of *PowerCtTabular* is to handle the interpolation of the power and Ct curves. This class takes as input a vector of wind speeds, a vector of power and a vector of Ct and returns a *powerCtFunction* function that calculates the power and Ct by interpolating the values provided. It also takes as input the interpolation method that can be *linear* or piece-wise Cubic, *pchip* or *spline*.
In the calculations, we opted for linear interpolation as it is faster without introducing significant errors, as these are known and smooth curves, without particular points of discontinuity.[71]

The analyses will be carried out both for fixed turbine models and with the type of turbine model as a free variable. In this second case, the objective of the analysis is to verify whether a configuration with mixed-type turbines can be more favorable than a single-type configuration.

4.3 Implementation of the *LCOE*, calculation and hypothesis

As already mentioned, the performance evaluation of the array can be carried out by directly considering the *Annual Energy Production (AEP)*, measured in $GWh/year$. This parameter is extremely indicative as it depends directly on the energy of the resource, i.e. how much wind is available in the area, and on the interaction of the turbines in the wind farm. In fact, if the turbines hinder each other, and the aerodynamic field is inefficient, the annual producibility of the array decreases.
Ultimately, an optimized spatial arrangement results directly in higher annual energy production.

In light of this, it is clear that the *AEP* is a fundamental parameter to consider in the design of a wind turbine array, but more generally for any power generation plant. Even just to define its order of magnitude. However, it is not certain that it is or should be the only parameter taken into account. In fact, ultimately, what is decisive in the design choices is not directly the producibility but the cost necessary to sustain to produce the energy; that is, the levelized cost of energy, *LCOE*.

The *LCOE*, is a preferable parameter to the *AEP* because, in addition to optimizing the aerodynamic efficiency, it guarantees the economic optimization of the array. Namely, it is a parameter that synthesizes both and guarantees the right compromise between the two optimizations that often, as in this case, are in contrast with each other.

The evaluation of the *LCOE* is a complex calculation that summarizes conflicting needs.
Good producibility, which would determine a low *LCOE*, is obtained from a wide spatial arrangement where the interaction between the wind turbines is reduced.
On the contrary, even a lower initial investment cost would reduce the price of energy, and one of the items that make it up is the cost of electrical cables, where the shorter their length, the lower the cost. Therefore, opposite to before, it is a more compact arrangement that favours a reduction of the *LCOE*.
Specifically, there are two cables, the high-voltage ones that connect the off-shore array to the coast, whose cost is independent of the position of the individual turbines, and the medium-voltage cables, whose role is to connect the various turbines to the offshore station for the subsequent increase in voltage. It is this latter type of cable that varies in length depending on the position of the turbines. And as said, the closer they are, the shorter their length. It follows that the initial investment cost tends to decrease as the spatial distribution of wind turbines is more compact.
In other words, an influence on the *LCOE* opposite to the one seen before.

As we have seen, the two main optimizations synthesized in the *LCOE* tend in opposite directions and the evaluation of this parameter is the best and simplest way to obtain the most convenient compromise.

As always, do not forget that for an overview, other parameters including those that make up the *LCOE*, will have to be taken into consideration.

For the calculation of the *LCOE*, many hypotheses and some preliminary calculations are made. The quantities that contribute to the calculation of the *LCOE* are the costs and the energy produced annually. Within the algorithm, the following formula is implemented:

$$LCOE = \frac{\text{CAPEX} + \frac{\text{decom}}{(1+r)^y} + \sum_{i=1}^{y} \frac{\text{OPEX}}{(1+r)^i}}{\sum_{i=1}^{y} \frac{\text{AEP}}{(1+r)^i}} \quad [€/\text{MWh}] \tag{9}$$

[72] Where:

- OPEX; are the maintenance costs.
- decom; are the costs of decommissioning.
- r; is the discount rate.
- y; is the estimated operating time of the plant.

The **operating and maintenance costs** are significant in the life of a plant and can influence the value of the *LCOE* considerably. Those costs are considered as an annual expense; in fact, as for the *AEP*, the effect of the discount rate is considered annually thanks to the summation.

These costs vary considerably depending on the state of development of the technology but, even though it is a recently evolved technology, we will consider a value of 0.09 $M€/MW$ typical of commercially started technology.[73] This choice is justified by the fact that the maintenance differences between floating and non-floating offshore wind are minimal.

They typically include many types of operational activities such as employee training, ground logistics with lifting and overhead crane facilities and administrative structures, offshore logistics such as ships for personnel transfer and service operations, and helicopters. As well as software for weather forecasting and oceanic weather data. Communication equipment and health and safety equipment.
In addition, it also includes many maintenance operations such as maintenance and service of turbines such as Inspection and repair of blades, replacement of major worn components and maintenance of the electrical transmission system. As well as inspection and repair of anchoring cables and control substations.
Within this value, finally, also the costs of insurance expenses are included.[74],[73]

The **decommissioning** of an offshore wind farm is a process of dismantling and removing the structures and components of a park at the end of its useful life.

It consists of removing the wind turbines and their anchoring systems. In the deactivation of electrical devices, such as transformers and submarine cables. And in their transportation to the mainland, where they can be recycled, reused or disposed of. Finally, the marine environment

must be restored, through site remediation and monitoring of ecological impacts.

All this has considerable costs that in this analysis are estimated to be equal to 0.062 $M€/MW$.[75]

The **discount rate** is the rate of return that is used to discount future cash flows in order to consider the loss of value over time of money. It is very complex data because it also takes into account many other aspects such as the general economic situation, the returns of alternative investment opportunities and the real or perceived risks of the investment.

r is a value that technically varies over time but can be considered constant for simplicity of calculation. For calculations in the energy field, its typical values are between 3 and 12%. [72],[76]. However, there are many factors that influence it; "for example regarding political and regulatory developments, the market design, the system development and future investment and fuel costs"[77]. Therefore, investments in renewable energy would tend to reduce the risk related to policies against environmental impacts, but on the other hand, they see an increase in risk due to the lower predictability of electricity production.[77]
In the specific case under examination, moreover, we are considering a type of plant with floating generators; that is, a new technology to the market. This aspect led to a conservative choice of a discount rate of 10%.[72] However, precisely for this reason, it can be imagined that in the near future, lower discount rates can be considered up to values of 7%. [72]

y, that is, the **estimated operating time** of the plant is considered to be 25 years for this type of plants.[72]
In the calculation of the cost of energy, it consists of the time span over which to distribute the investment and moreover in the years in which the plant produces energy. In general, the higher it is, the lower the $LCOE$

Going into more detail in the calculation of the costs, the items that constitute them are:

- **Cost of wind turbines**; it is the most decisive parameter within the calculation of expenses. A cost of 1.3 $M€/MW$ is considered.[78] Therefore, the total nominal power of the wind farm is calculated and then the result is obtained.

- **Cost of floating platforms**; it is the second most relevant item of the calculation. Here too, a cost is considered based on the unit of power, so the procedure is identical to the previous one. The platforms vary depending on the type of flotation. For these turbines, as anticipated earlier, a consolidated type of spar buoy was chosen at a cost of 0.51 $M€/MW$.[79]

- **Installation cost**; this item condenses the costs of all the phases of the installation that range from rental of specialized vessels for the transport of the turbine and the foundation, specialized personnel, to fuel costs, port costs and charges for the site.
  In addition, the cost of commissioning and testing the turbine and the foundation must be considered, which depends on the current regulations and quality requirements.
  As above, the calculation is performed considering a cost per unit of power of 0.42 $M€/MW$.[79]

- **Cost of electrical cables**; as discussed earlier, there are two different types of cables with their respective costs. High and medium voltage and this item contains both, along with the costs of the transformer, cost of connectors, cost of safety devices (SwitchGear).
  Specifically for this analysis, these last two, together with the costs of the high voltage cables

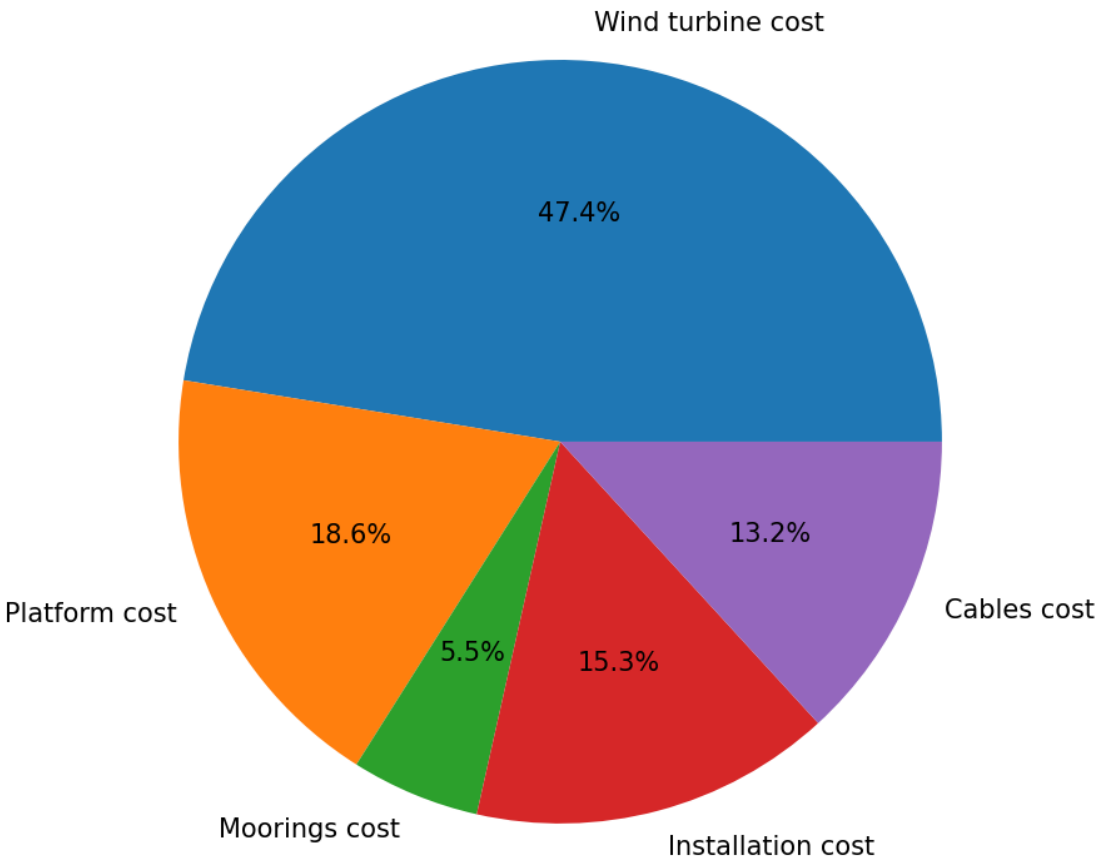

Figure 9: Off-shore floating wind turbines farm, costs

are considered constant for each possible configuration of the wind farm and number of wind turbines, with a cost of 23 $M€$.[80] And this is because it was assumed to use an area 20 km away from the coast.
On the contrary, the cost of medium voltage cables, as discussed earlier, depends on the position of the individual turbines and is calculated based on the assumption that they have a price of 440 $€/m$ including installation. These values are referred to as a voltage of 33 kV and a cable section of $95mm^2$. However, considering that in the calculations of this thesis, I will not evaluate the specific section of the cable as the energy produced varies, I conservatively correct this value by multiplying it by a factor of 1.3.[80]
Finally, the cost of the transformer is considered proportional to the power by a factor 0.15 $M€/MW$.[81]

- **Cost of the mooring system**; it is the cost to ensure the stability and fixity of the generators. Different types of cable and in different numbers can be used, depending on the type of floating system. For the type of turbine used in this study, a spar buoy, three cables are used whose cost varies depending on the depth of the seabed.
  As stated above, in our site is reasonable to consider a depth of 180 m which corresponds to a cost per cable of 0.31 $M€/cable$ that becomes 0.93 $M€/turbine$.[73]
  The mooring system cost also includes the cost of the anchors, which amounts to 0.13 $M€/turbine$ for gravity anchors.[79]

5 Results obtained

5.1 Analysis for single and mixed turbine models

This chapter presents the results obtained and describes in detail the conditions under which they were calculated.

The data are then analyzed and evaluated. Where appropriate, interpretations and explanations of trends and behaviors are also given.

The calculations are classified into two categories: those that evaluate the performance and optimization of configurations with the same turbine model, and those that compare different turbine models to assess the benefits of their mixing.

5.1.1 Optimal wind turbine number, changing the domain

The main objective of this first study is to determine the optimal number of turbines of the same type for a given domain.
We considered square domains with surface areas of 4, 9, 16 and 25 km^2.

Figure 10 illustrates the optimization for two sets of curves: model *Small* and model *Big* turbines, presented in section 4.2.3.
This graph aims to demonstrate the relationship between the $LCOE$ values of the two families of curves.
However, to better compare the different behaviors across the domains in the single set of curve, the two are plotted separately in the following two graphs.

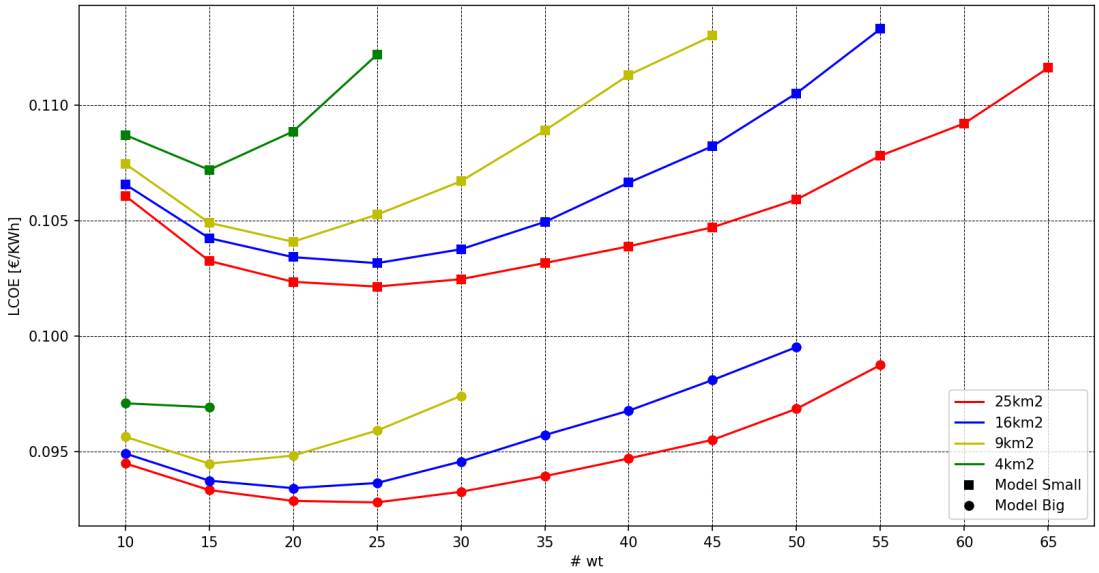

Figure 10: Optimal number of turbine for both models

This analysis involved finding the optimal layout for each possible configuration. This means that each point on the graphs represents a genetic optimization outcome.

To ensure the consistency of the results, all the points and curves were obtained using the same settings for the genetic algorithm; namely, creating 150 individuals per generation, for 300 generations.
To minimize the statistical error, the curves shown are the average of two simulation runs. Obviously, two is not an adequate number to reduce the statistical error significantly, but the computational time required for these curves prevented us from doing otherwise.

All the curves were computed until the maximum number of turbines that could fit in the domains was reached. This means that the graphs also indicate how many turbines of a given type can be placed in the domains.
For instance, no more than 50 model *Small* turbines can fit in a 16 km^2 domain.
The Penalties discussed in section 4.1.2 played a crucial role in this result. In particular, in this simulation each turbine had to keep a minimum distance from the others equal to 1.5 times its own diameter; and this means a total distance between one turbine and another of three times the diameter of the chosen turbine type.
To ensure the consistency of the results, this setting was used for all the simulations of the graphs in this chapter.

For all the graphs in this section, we chose to optimize for a fixed number of wind turbines; starting from 10 and increasing by 5 each time.
This choice was driven by the very high computational times that limited a more detailed analysis. Therefore, we cannot determine the exact optimal number of wind turbines, as it might be in between the chosen steps. However, this analysis is still very interesting, as it reveals trends and general values.

The graph in fig. 10 is useful to show the relationship between the two sets of curves; the first one, corresponding to the simulations with the turbine type that in section 4.2.3 is been called *Small*, and the second one, corresponding to the simulations with the turbine *Big*.
The main difference between the two turbine models is power. This results in a higher energy output, and therefore a lower *LCOE*. This can be easily seen by comparing the two sets of curves. Furthermore, it can be observed that for each domain size considered, the maximum number of turbines that can fit is always higher for the set of curves corresponding to the turbines *Small*, than for the set of curves corresponding to the *Big* ones. This is due to the difference in their diameters. Smaller diameters allow for a better packing, enabling more turbines to participate in the simulation.

Anyway, the main result that emerges from these curves is their minimum point. It can be seen that all the curves have a point that, corresponding to the lowest value of the *LCOE*, it tells the optimal number of wind turbine for each domain.
However, for a better understanding of the optimal configurations and the trends in between the family, we will refer to graphs in fig. 11 and fig. 12 from now on.

Considering the family of curves for the turbine type *Small*, one can observe a trend of increasing the optimal number of wind turbines as the size of the domain increases with a variation of the optimized value of *LCOE* from the smallest domain to the largest one of 5 €/*MWh*. A similar trend is also found for the type *Big*. For which, the difference between the optimized values between the curves of the two largest and smallest domains is higher than 4 €/*MWh* and close to 5.

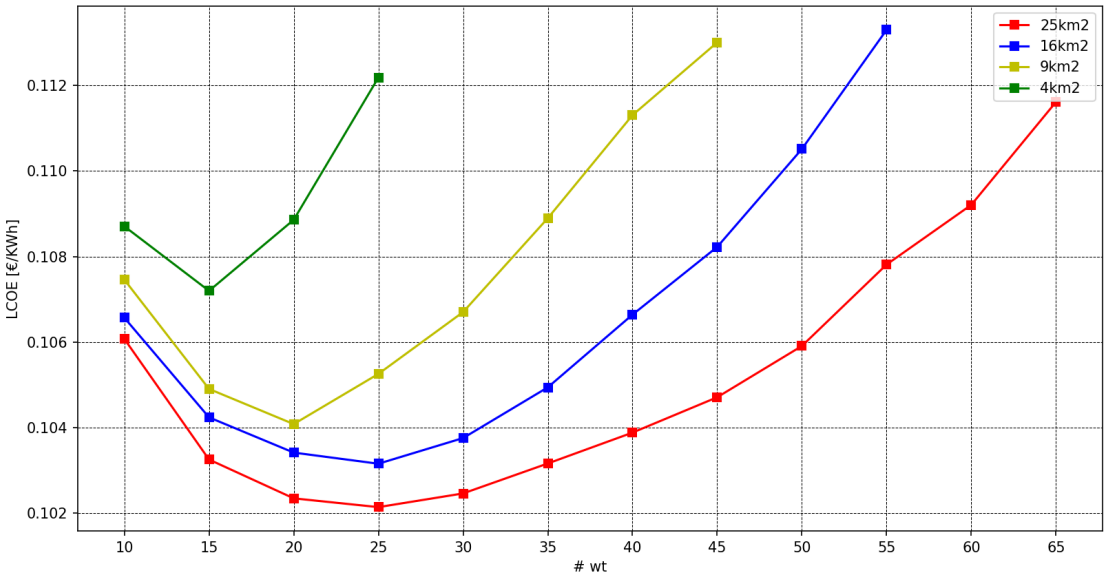

Figure 11: Optimal number of turbine for model *Small*

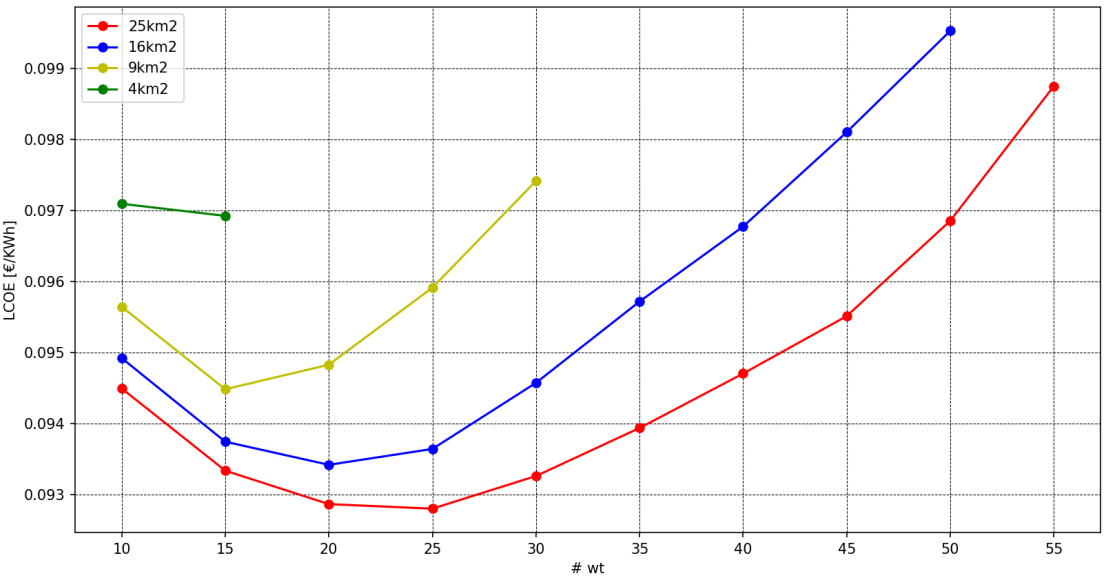

Figure 12: Optimal number of turbine for model *Big*

The presence of a minimum point for all the curves is a factor of great interest because it identifies an optimal number of turbines to be inserted in each domain.
Moreover, the fact that there is no indiscriminate reduction of the *LCOE* as the number of turbines increases indicates that the shading effects of one turbine on another increase as the number of turbines increases. This because it becomes increasingly difficult to arrange them in an optimized way.

Furthermore, the fact that at first the value of the *LCOE* decreases as the number of turbines increases, means that the contribution of the added turbines is favorable; that is, that the increase in shading is not enough to nullify the addition of the energy produced (we are not directly analyzing the *AEP* but the *LCOE*, of which the former is only part of the calculation).

The observations made so far concerned the production side, but not the economic one. However, further explanations on the initial behavior of the curves may lie in the method used to calculate the *LCOE*.
Indeed, as explained in section 4.3, the calculation is divided into fixed and variable quota depending on the power of the farm. This means that, whatever the power of a wind farm, there is a fixed price to pay in order to proceed.
It follows that the fixed quota is hardly amortized by small plants, and more easily by larges. Therefore, by increasing the number of turbines, even if the variable quota of the plant price consequently increases, the fixed part of the capital cost is more easily amortized because it is spread over more devices. Trivially, the energy produced increases more than the increase in the initial investment. That is, the levelized cost of energy is reduced.
This behavior is similar to that obtained by the economy of scale. In this case it is difficult to define it as such because there is no standardization of processes and it cannot be affirmed that the increase in the number of wind turbines does not entail further variations also in the variable quota of the capital cost.

Having analyzed the favorable and unfavorable effects that govern the trends of the curves, it can be summarized that: for both families of curves, the configurations with the lowest number of turbines are disadvantaged by the fixed cost quota considered in the *LCOE*. Then, by increasing the number of turbines, the increase in energy production that results prevails over the increase in initial investment and even allows to amortize it. Finally, with the further increase in the number of wind turbines, the increase in production that results is no longer necessary to amortize the initial investment. The *LCOE* returns to increase because the prevailing effect is the opposite one of wake that reduces its efficiency.

In the graphs in fig. 11 and fig. 12 it should also be observed the shift of the minimum points to the right as the domain increases.
It is a phenomenon that affects both families of curves and can be understood by observing that increasing the size of the domain, the optimal number of turbines of the ideal configuration increases with it.
This shift of the curves is consistent with what can be expected. As said before, the increase in the number of turbines helps to amortize the initial investment, but a domain of reduced size is not able to accept a high number of wind turbines. Consequently, as the size of the domain increases, the optimal number of turbines to be inserted increases and with it the amortization of the fixed quota.

5.1.2 Analysis of the relationship between best wind turbine number and domain dimensions

Given the results obtained from the previous graphs, another interesting information to derive and analyze is the relationship that exists between the number of turbines and the size of the domain. Figure 13 shows the trend of this relationship for the two types of turbines in the various domains.

The calculation is performed based on the results shown in fig. 11 and fig. 12. In fact, for each type of turbine and domain, the optimal number of wind turbines defined by the optimization is selected, and its ratio with the domain is calculated.
We call this quantity *Wind turbine density* because it is the ratio $[\frac{wind\ turbine\ nominal\ power}{Domain\ dimention}] = \frac{MW}{km^2}$.

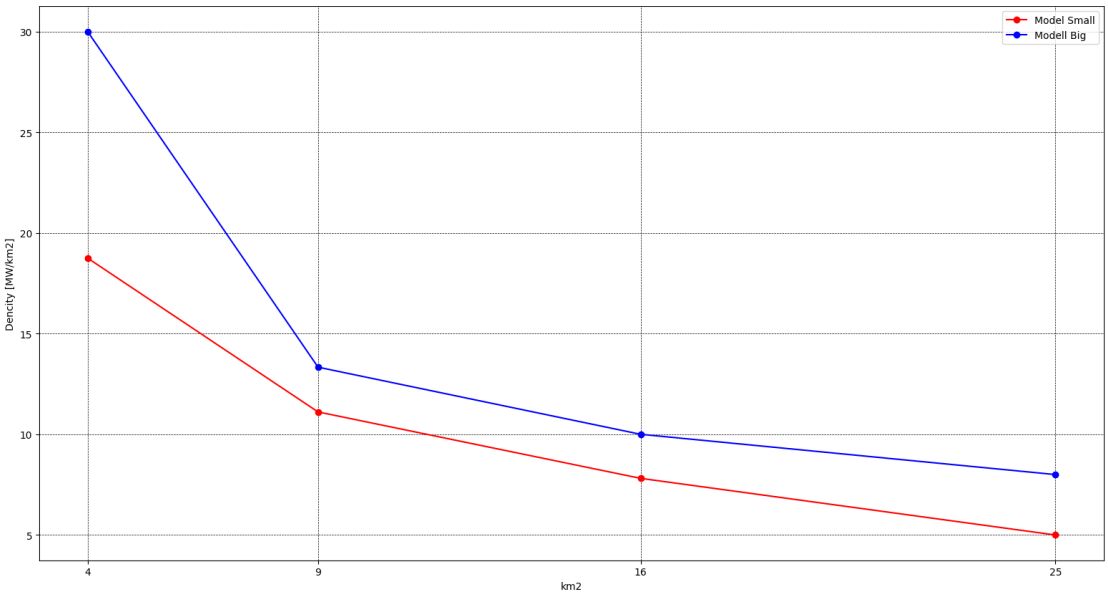

Figure 13: Optimal wind turbine number density

The graph in fig. 13 shows a downward trend as the domain size increases for both curves. This means that the ideal number of turbines per unit area decreases as the domain grows. Consequently, the ideal configuration for a growing domain is with turbines arranged in a less compact way.
This result is not in line with the expectations. One could observe that the relationship between the different turbines is not necessarily related to the domain size, so it could be expect a linear trend independent of the domain. Or, that a larger domain should allow a more free arrangement, favoring the aerodynamic performance of the wind farm, and thus a better packing and hence a higher density.
On the contrary, the trend of the curves is decreasing, indicating a higher packing for the configurations with smaller domain.

The values shown in the graph can be explained first of all considering that the largest is the turbine number and the higher is the shadowing, then by interpreting them as consequences and not as causes.
The limited size of the smaller domains dictates their ideal turbine densities. Adding more turbines would result in penalties. As shown in the curves for the $4km^2$ domain in fig. 12, the ideal turbine density is high and decreases with every additional wind generator.

The observations mentioned earlier, which seem to contradict the graph in fig. 13, are actually realistic. They determine the ideal densities for larger domains. The validity of these densities is confirmed by the corresponding $LCOE$ values for these optimal configurations, which are lower for larger domains, although they produce greater wake effect. [82]

In conclusion, the trend of the turbine density is dictated primarily by the domain size and the penalties applied. It does not provide a trend that can be extrapolated for other domains and sizes.

5.1.3 Evolution of one of the optimizations for a specific wind turbine number in a specific domain

All the graphs presented in this section represent the wind map for the same wind turbine configuration, that is, the same model of wind turbines, the same number in the same domain, with the same types of penalties, but at different moments during the optimization. Turbine type *Small* in a $9km^2$ square diameter.

Unlike the previous graphs, in this case, being an isolated simulation, it was possible to perform a more in-depth and computationally costly optimization. This means that a larger number of generations were simulated, for a total of 400, using the most accurate and highest computational cost calculation model discussed in section 4.2.1.

The graphs show eight different moments during the optimization. They are not evenly distributed because we preferred to highlight more the significant differences during the evolution. Considering that in the first half of the evolution the changes are marked and frequent and that in the second, approaching the plateau, they become more difficult to appreciate, there are more snapshots of the first than of the second half.

All the graphs presented in this section depict only one wind direction, the 315°, even though we performed the simulation for all directions simultaneously.
We preferred to execute the graphs to favor the visualization of direction with the highest producibility, and therefore the highest *LCOE*. That is, the dominant wind direction.

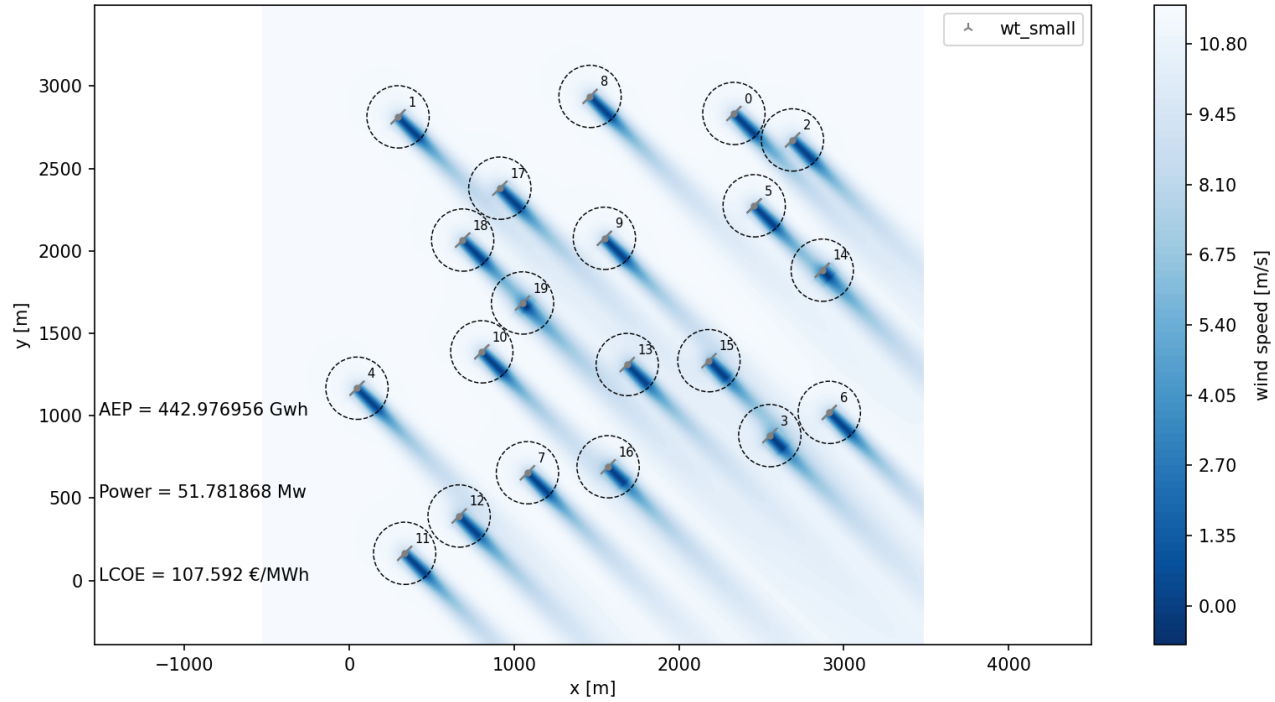

(a) Generation 1

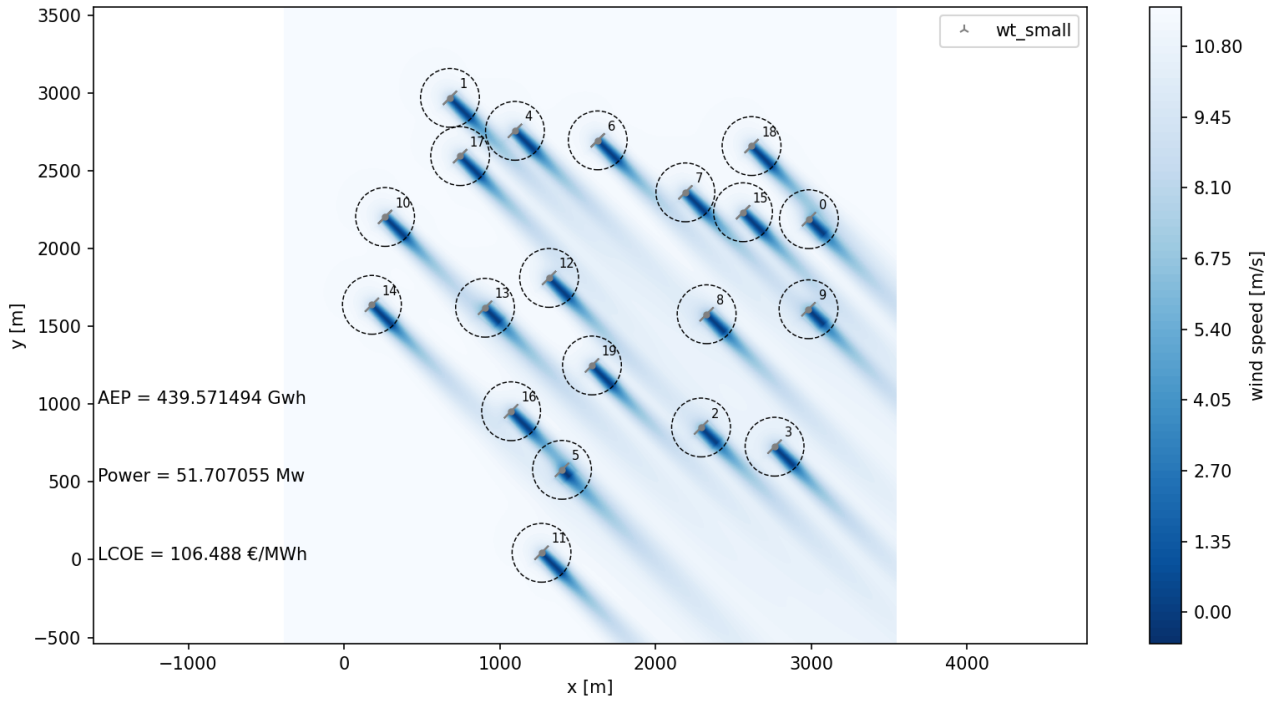

(b) Generation 5

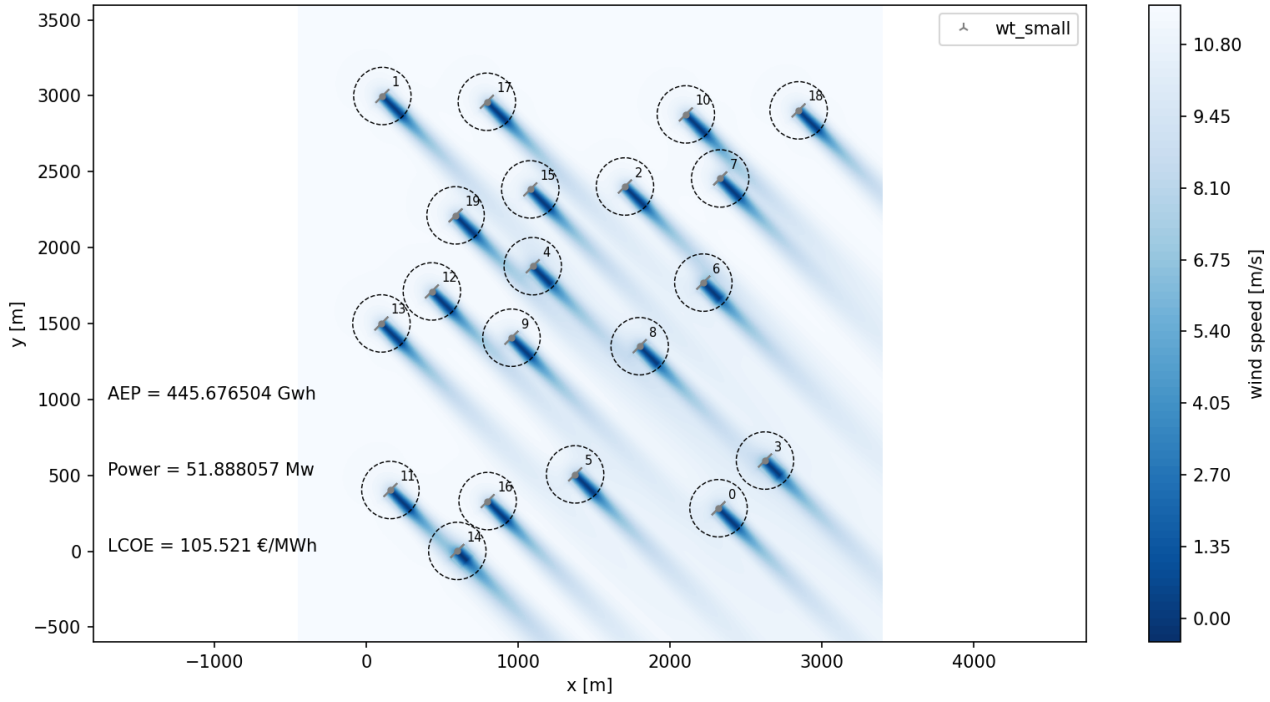

(c) Generation 30

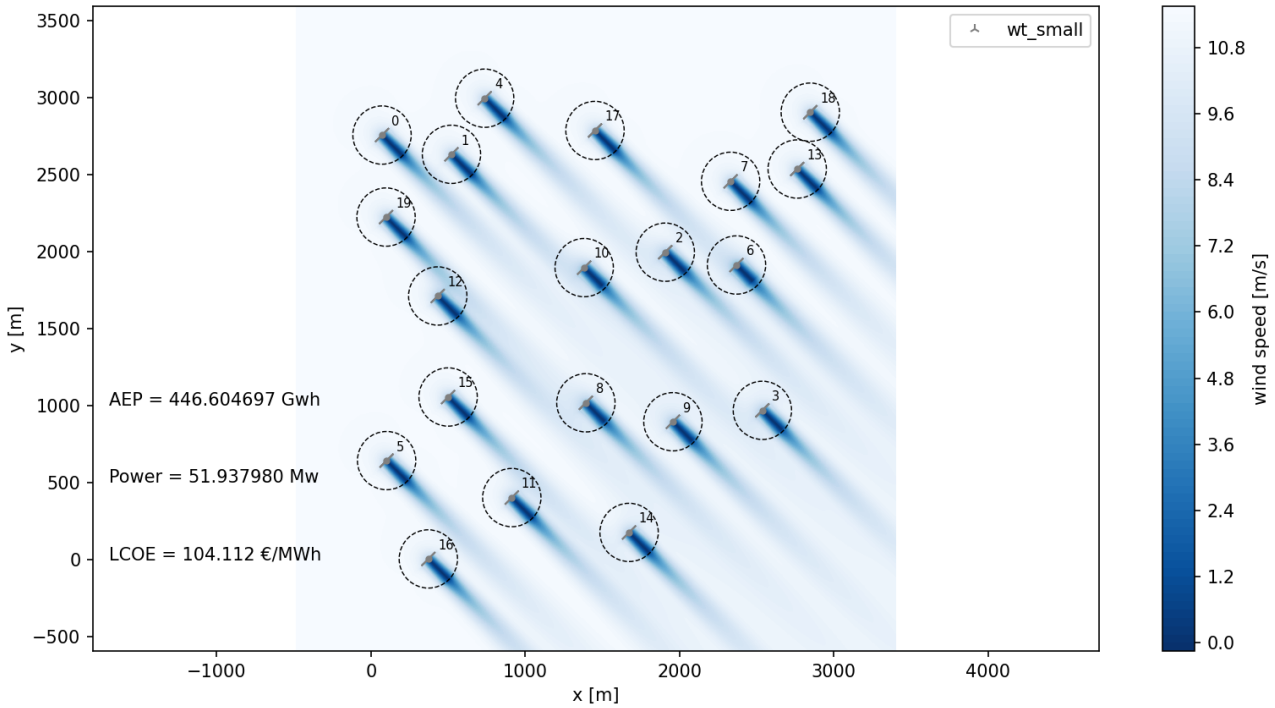

(d) Generation 65

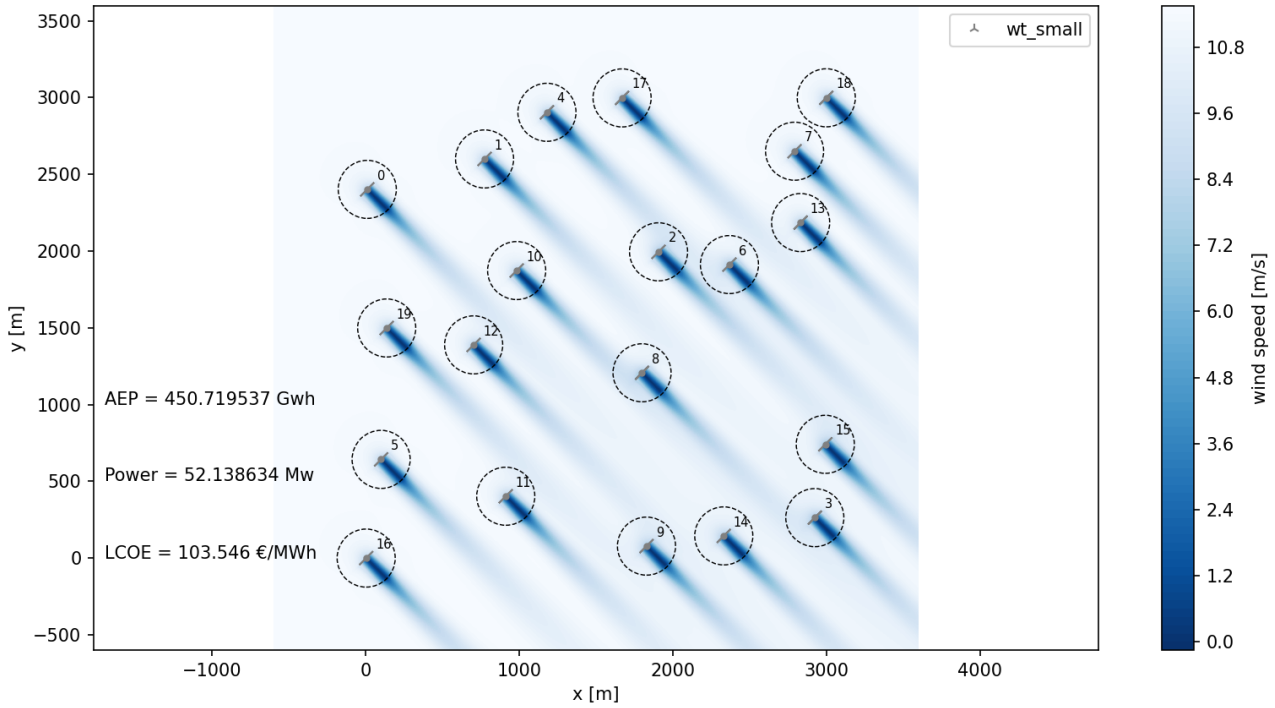

(e) Generation 120

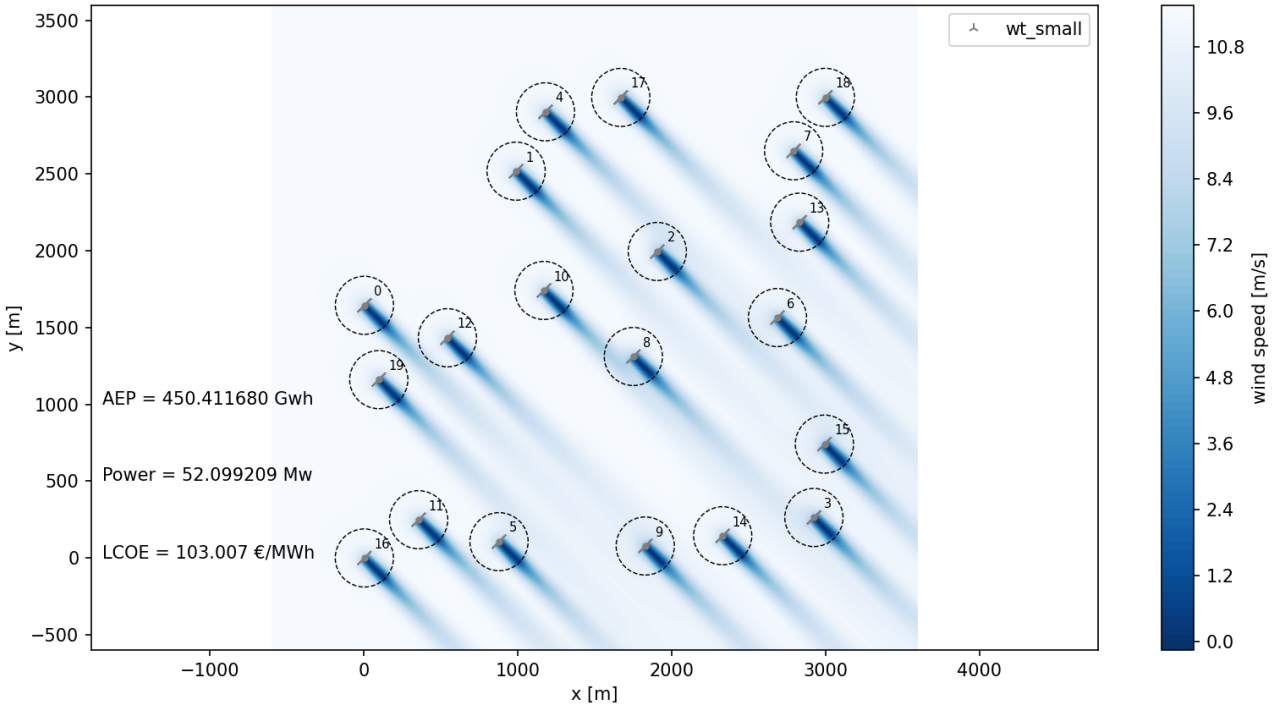

(f) Generation 200

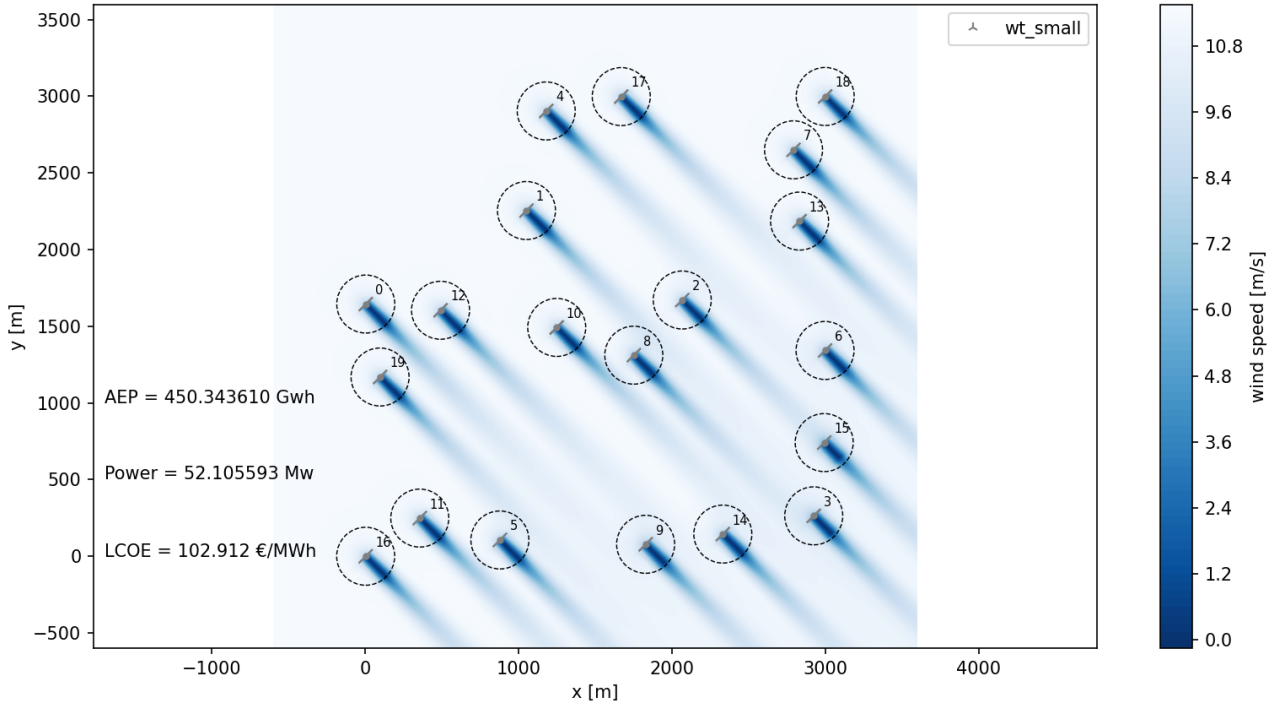

(g) Generation 300

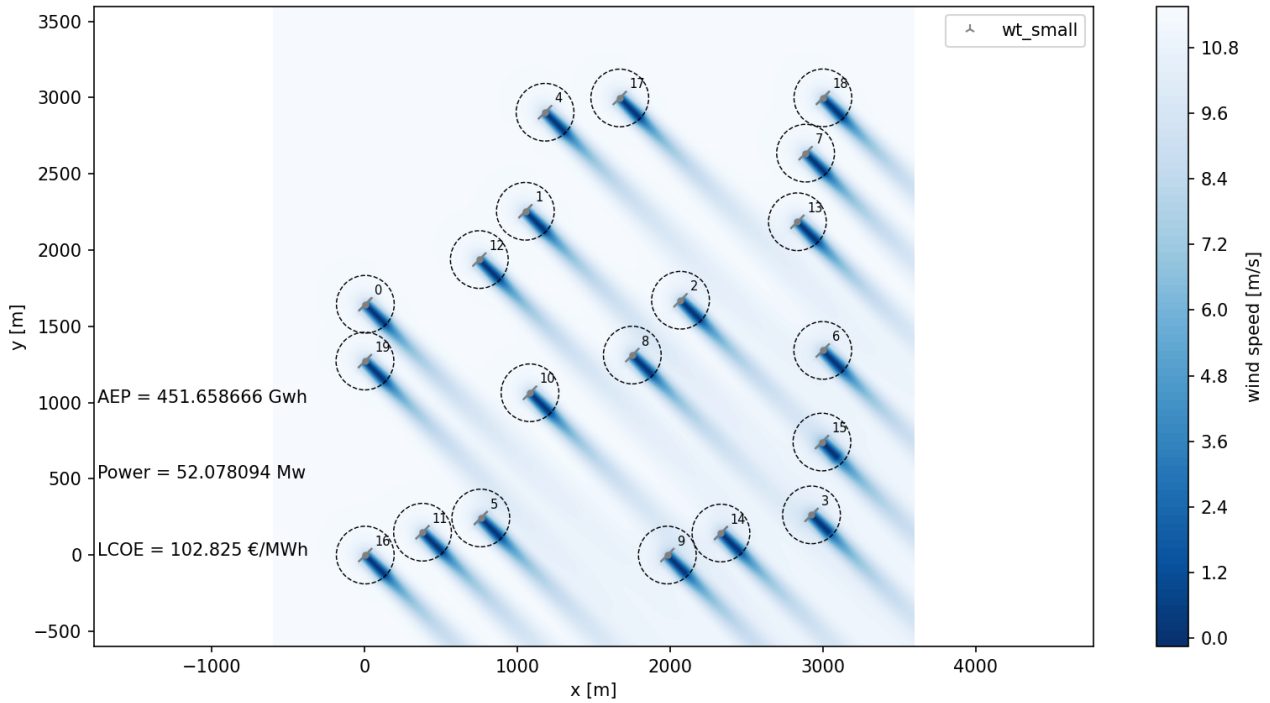

(h) Generation 400

Figure 14: Optimal individual evolution during genetic algorithm

Specifically, the graphs represent the wind map in the wind farm; that is, the wind speed and its perturbation due to the wind turbines.
On the right, the color-bar is always shown. The dark blue represents a low-speed wind, while the lighter the color, the higher the wind speed represented.
The distribution of the shadows due to the wind turbines and their evolution in space are the result of the application of the models chosen to compose the calculation model used, which we discussed in chapter section 4.2.1; that is, the *BastankhahGaussianDefici*, the *SelfSimilarityDeficit*, the *STF2017TurbulenceModel* and the *GaussianOverlapAvgModel*.

As we explained in section 4.1.2 introducing the penalties, in the calculation we first compute the potential penalties of each configuration before calculating their aerodynamic performance. We only perform the performance calculations for configurations with no penalties. This means that the layouts need some initial adjustments during the first generations. It would not be very useful to show these layouts, since they do not have any aerodynamic calculations. It usually takes about ten generations to overcome the penalties.
We define generation 1 as the first generation that has an individual with no penalties and that has been evaluated for its performance.

By analyzing the graphs presented in fig. 14, it is possible to appreciate how the best individual changes in different generations during the optimization.
Attempts have been made to select some remarkable moments of evolution.
Initially, in the first generations, the arrangement is almost random and also the changes between one generation and another do not follow a precise pattern. This is due to the low level of optimization, which sees in every variation a consequent improvement, without having to follow specific schemes.

Continuing with the optimization, it will be seen that at high levels of optimization it is very difficult to obtain further improvements and that only individuals who bring variations that increase the symmetry or the homogeneous exploitation of all the areas of the domain are saved.

In fig. 14a, fig. 14b and fig. 14c it can be seen that there are no particular correlations between the arrangements. It can nevertheless be analyzed how the *LCOE* values reported in the graph follow the trends shown in fig. 17 and analyzed in section 5.1.5.

However, it must be considered that the graph in fig. 17 was produced by simulating the aerodynamic behavior through the calculation model less precise and more conservative shown in section 4.2.1. On the contrary, the evolution presented in this section was obtained with the most precise aerodynamic calculation model. This difference translates into a discrepancy between the results of 1 *€/MWh*.
For example, the optimized value at generation 300, has a value of 102.825 *€/MWh* for the most precise model, fig. 14g. And an approximate average value of 104 *€/MWh* for the more conservative model used in fig. 17. This discrepancy was expected and is discussed in section 4.2.1.
Each graph reports the generation to which it corresponds and the *LCOE* value. The consistency of the data can be evaluated by comparing them with the data shown in fig. 17 minus a constant $a = 104 - 102.825$ *€/MWh*.

From the graph in fig. 14d it is possible to start seeing a group of turbines in the upper left corner that will remain in that area for all future generations. Among the turbines that in the final version will not undergo drastic changes, we can include the 1, the 4 and the 17. In the upper right corner the 18 together with the 8 and the 13 that will later reverse. In the lower left corner the 16.

From this graph it can be deduced that initially, the algorithm tended to place the turbines as close as possible to the area most favorable to the wind dominant direction; *north-west*, i.e. in the upper left corner. From the next generation presented in fig. 14e, the complementary trend is found. Once the resource is exploited by the first line, there is an advantage in placing the wind turbines far enough away to regenerate the air flow. From generation 120 onwards, in fact, there is a group of turbines in the lower right area, which will consolidate for all subsequent generations. In this last graph it is also possible to appreciate the formation of the trio of turbines in the upper right corner that will be maintained with minimal alterations until the final generation.

Figure 14f depicts the generation 200 and shows the tendency of the turbines to group together in small groups. In addition to those born in the generation discussed above, there is a group in the lower left corner of the turbines 16 11 and 5 that will remain such in the final version.
Moreover, a central group and two other lateral groups with the turbines 0, 19 and 4, 17 are outlined.

Between the generation 300 and 400 shown respectively in fig. 14g and fig. 14h, the differences are not remarkable despite the 100 generations of difference between the two. This is explained by the plateau that is created from generation 150 and that can be deduced to extend until generation 400, shown in fig. 17.
In these two configurations, the conclusion of the backward movements of the turbine 6, the lowering of the 1 and the 10 and the centralization of the 12 can be appreciated.

The graph that shows the optimized configuration is discussed in more detail in the next section.

After analyzing the overall scenario, we can notice that turbines 18 and 16 achieve their final positions much earlier than the others. The former does it in generation 5. The graph in fig. 15 shows that turbine 18 has the highest productivity, followed by turbine 16. We can speculate that there is a correlation between these facts; that is, the high productivity of these locations has ensured that the turbines were included in every high-performance layout within the generations.

It should be remembered that the genetic algorithm is a stochastic analysis and, therefore, the result it produces should follow some trends, as discussed later in section 5.1.5. However, the final result is hardly repeatable, and it would hardly produce a similar arrangement to the one presented in this chapter. Several evolutions have been performed, and the most interesting one among those obtained has been presented.

5.1.4 Layout of the optimized disposition for the optimized wind turbine number in the chosen domain

The previous section showed how the layout of the wind farm changed during the genetic optimization process in fig. 14. In this section, are analysed in detail the final outcome of the optimization reported in fig. 14h.

The figure shows the optimal layout of 20 wind turbines of model *Small* in a $16km^2$ area.
As we mentioned before, we used the second calculation model for this optimization; that is, the more precise one. And as we also explained, we only show the wind map for the prevailing wind direction; that is 315°.

The graph in fig. 14h shows a symmetrical layout of the wind turbines after the optimization. This symmetry follows the prevailing wind direction, 315°, which matches the values shown in fig. 5.
We can see that the layout meets the requirements imposed by the penalties.
Also, it can be seen how this arrangement avoids or at least reduces the overlap of the shadow wakes, especially in the main wind direction (indicated in the graph), especially compared to other moments of evolution reported in the other graphs in fig. 14.

For instance, look at how close turbines 0 and 19 are. Even though there is room to separate them, for example by lowering the y coordinate, this would affect the exposure of turbine 5 negatively. Or, look at how the turbines in the middle section of the domain along the dominant direction, (turbines 1 and 12 and those behind them) are all staggered.

There is a lot of empty space in front of turbines 1 and 12. Nevertheless, we can presume that placing a turbine there would have a negative impact on all the wind turbines behind it, resulting in a net loss of performance.

Finally, let us make a consideration on the optimal values obtained. An *LCOE* of 102.852 *€/MWh* is still remarkable compared to the trends for latest generation offshore wind farms. However, It has to be consider that the site under analysis in this thesis work has a lower availability of the resource than the ocean sites where offshore plants are more common. The *LCOE* obtained is high, but not out of scale.
As for the *AEP*, the optimized result is 451.6 *GWh*. Calculating its Capacity Factor according to the formula: $CF = \frac{Energiy\ produced}{Energy\ theoretically\ produced}$,with the energy theoretically produced calculated as if

the nominal power of the plant was fully and continuously exploited: $5MWX20turbinesX8760h = 876GWh$. From which a CF of $0.51 = 51\%$ is obtained.

This value is satisfactory because it is very high for a wind farm, but in scale for offshore ones.

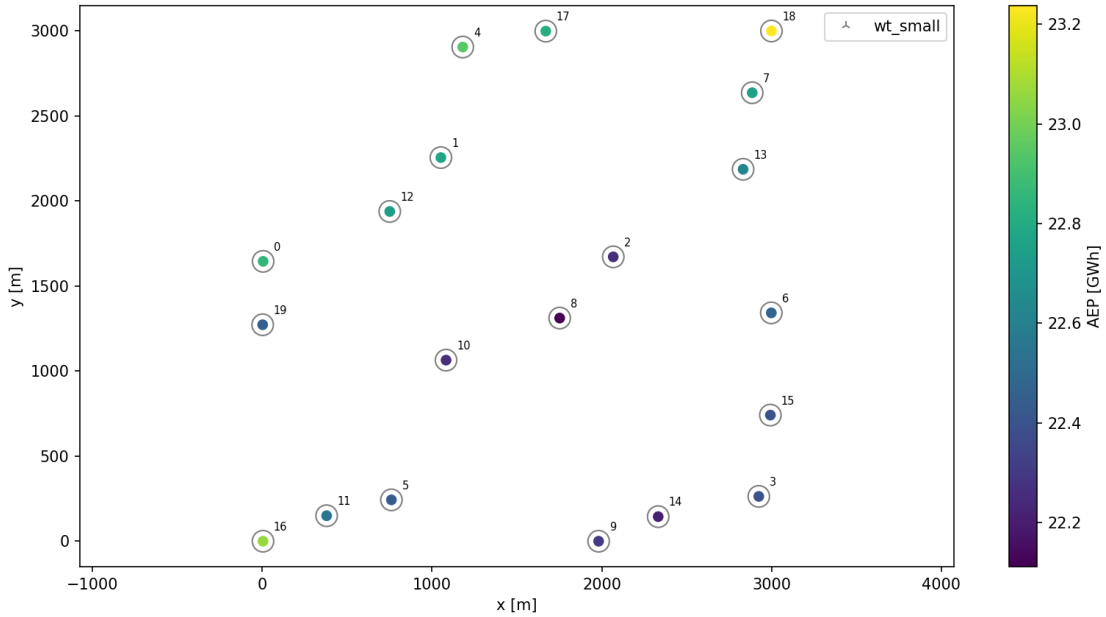

Figure 15: AEP values for each turbine

Figure 15 displays the AEP values for each turbine, contributions are cumulated from each direction.

We should point out that the AEP is not the main goal of this analysis; that is, indeed, the $LCOE$. However, this last is a global measure of the wind farm. It cannot be broken down into the individual contributions of each turbine. On contrary, AEP is a value of each turbine. Therefore is a good proxy for the $LCOE$ since they are part of its calculation.

This final graph provides useful information about which wind turbines have the best and worst productivity. Therefore, they suggest which ones we should pay more attention to in order to improve their position and, ultimately, which ones we should consider removing.

As expected, the turbines with the best productivity are those in front of the others along the dominant wind direction.

Observing the symmetry discussed in the previous lines, one can see how the right half has better performance. For example, comparing the already discussed turbine 19 with its counterpart 17, where the latter can boast a higher productivity.

Always referring to fig. 15 one can deduce which turbine is the most productive; it is number 18.

In fact, it has the front free with respect to the main direction of the wind, so it is not surprising that it has an excellent performance. However, this is not enough to explain why it stands out so much compared to the others that, like it, have no obstacles in front.

This is explained by the fact that the position of turbine 18 is particularly favorable also for the other wind directions, which, for many of the other turbines, are neglected.

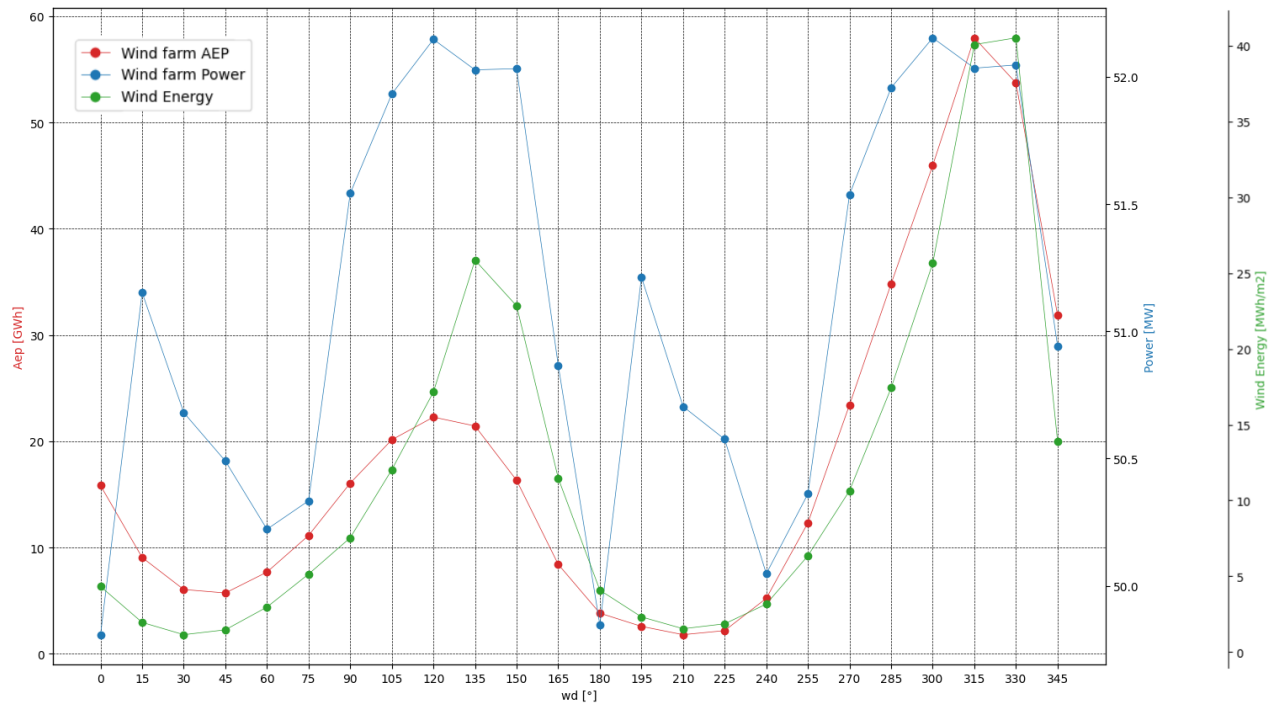

Figure 16: Wind farm Directional analysis

The graph in fig. 16 is very interesting and articulated. It depicts the *AEP* with the 24 wind directions discussed in section 4.2.2 on the x-axis. Therefore, it studies the performance of the wind farm in the different wind directions.

It contains three curves: the *AEP*, the power of the farm and the energy of the wind, all divided into the different contributions of the different directions.

The idea of the graph is to show the *AEP* as a synthesis of the relationship between the site and the farm.
In fact, the contribution of the site is given by the green curve of the wind energy, the contribution of the farm is given by the blue curve representing the power of the wind farm. The red curve, finally, represents the *AEP*, that is, the energy produced as a result of the relationship between the energy available at the site, and the power of the wind farm.

The power of the farm is an output of the calculations performed with the PyWake library. The simulation, in fact, returns the power values for each turbine, for each direction and speed of the wind. By summing appropriately the different values, one obtains a vector of 360 elements, as many as the wind directions with which PyWake works; averaging them over the 24 sectors on which the input data of the site are organized, is obtained the blue curve.

The energy of the site was calculated with the following formula: $P = f\rho V^3 = [MWh/m2]$, where $\rho = 1.225\ kg/m3$ is the density of the air, f is the vector of frequencies and V the vector of average speeds, already calculated previously to provide the values of A,k and f as input to the function to model the site in PyWake, from the initial database.

The *AEP*, finally, is the main output of the analysis part that uses the PyWake library.

Comparing the curve of the site energy of fig. 16 with the wind rose of fig. 5 one can see how

the information is consistent with each other. The green curve has two maximum points at 135 and °, while, it degrades rapidly in the ranges $0 - 105°$ and $165 - 270°$; same behavior found in the wind rose.

According to what has been said so far, the green curve depends on the site and is independent of the arrangement of the turbines. The blue one depend only on the relation between them. The red curve of the *AEP* is the synthesis of the other two. The optimal condition for the *AEP* is obtained with a wind farm suitable for exploiting the energy available at the site. That is, for a wind farm that facilitates the wind directions with the highest energy content.
Therefore, referring to the values present in the graph, a wind farm is optimized if the values of its power per fraction of direction are high for the directions with the most available resource.
More generally, an arrangement is optimized if the curve of its directional power follows the trend of the directional energy of the wind.

In this case, in the graph reported in fig. 16 one can see how the result of the optimization has brought the curve of the power of the farm to resemble the curve of the availability of energy. In fact, the maximum points coincide, and both decrease in the directions far from the maximums. And this to produce a better *AEP* curve.

5.1.5 Convergence analysis for the given studies

The graphs in fig. 10, fig. 11 and fig. 12 were performed by averaging the results of two different simulations to reduce the statistical error. Nevertheless, the procedure cannot be said to be rigorous; the number of simulations to be performed should be greater. This was not possible due to the high computational cost of such simulations.
However, to validate the previous calculations, a convergence analysis was performed for only one of the previous curves. That is, the convergence was calculated for the optimization of the spatial arrangement of 20 model *Small* wind turbines in a $9km^2$ domain.

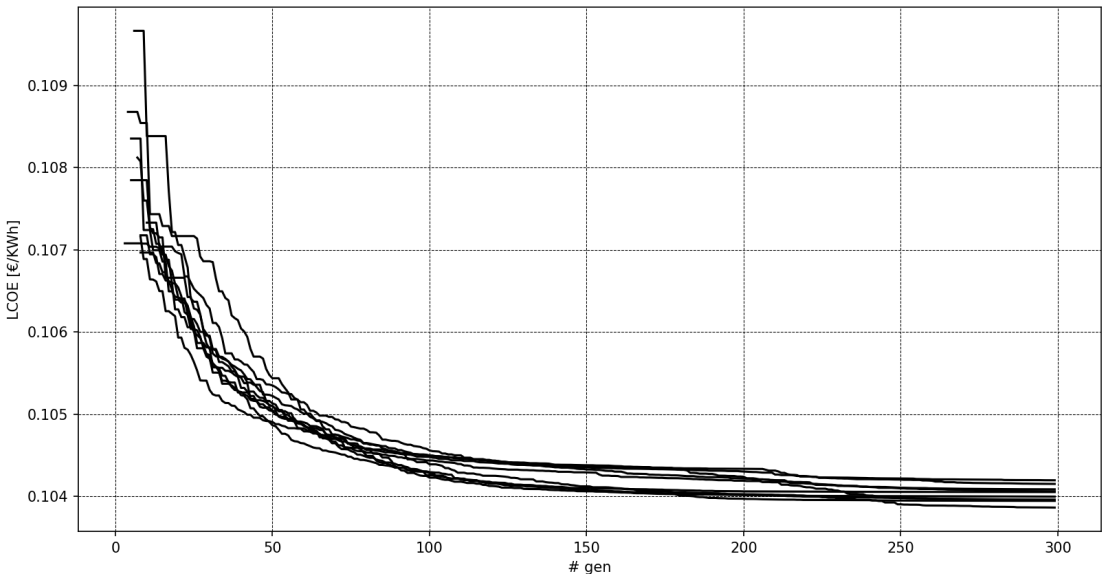

Figure 17: Convergence analysis for 25 wt model *Small* in a $16km^2$ domain

Figure 17 shows the convergence analysis for one of the curves of the graphs discussed earlier, assuming that it can represent the convergence of the other curves calculated as well.

To obtain this graph, 10 different simulations were performed to optimize the same type of configuration.
As for the previous curves, the simulation used 150 individuals for 300 generations, considering the calculation of penalties for a minimum distance of 3 diameters between one turbine and another.

As you can see from the graph the convergence is remarkable.
The curves start from high $LCOE$ values such as 109 or 108 $€/MWh$, and then converge to values around 104 $€/MWh$. More precisely, to an average value of 104.02 $€/MWh$. This coincides with the values shown in fig. 11 by the yellow curve for the optimization in the domain of $9km^2$, except for a difference of 0.6 $€/MWh$; a deviation of less than 1%.
Indeed, as already mentioned, the convergence graph is obtained by running the same code 10 times. Being heuristic simulations, the result cannot coincide. It can, however, converge to a result with a reduced variance; which happens in the graph in fig. 17. Since the setup of these simulations is the same as the minimum point of the optimization in the domain of 9 Km^2 (the aforementioned yellow curve of the graph in fig. 11), it is expected, as it is, that the convergence values and the value indicated by the minimum point coincide.

5.1.6 Varying turbine models

As discussed above, one of the objectives of this thesis is to evaluate the possibility of integrating several types of wind turbines into the same layout.
The idea is to verify whether, by operating at different heights, the space occupied by the turbines of one type is sufficiently different from that occupied by the turbines of the second type, to allow to increase the density of wind turbines, thus the energy production, and consequently whether the LCOE obtained is lower.

The two different types of turbines used are those discussed so far, whose characteristics are presented in section 4.2.3 and in table 1.
As can be seen, the difference in height is not significant, however these two models of turbines were chosen because real models were used and with a small difference in nominal power, to avoid that the larger model prevailed over the smaller one for a simple question of producibility.

In this calculation, an additional type of penalty was added to the penalties already discussed above to ensure that in each individual there were at least 1/3 of the turbines of both models, so as not to fall back into the simple simulation of type 2 turbines.

In fig. 18 one can see how the curves representing the mixed configuration are halfway between the two families of curves analyzed previously that refer to the turbine model *Small* and *Big*.
One can also see how the trends are similar among the three different configurations, presenting global minimum points. However, the trend of the last family is not smooth as for the previous ones, showing several deviations as for the optimization of 30 wind turbines in the domain of $9km^2$.
This behavior can be explained by comparing the families of curves of the *Big* and *Mix* models. The maximum number of turbines for the same domain, in fact, tends to increase in the second configuration. One can also observe that the trend of the *Mix* curves tends to the *Big* model for the simulations with low number of wind turbines, while it tends to the *Small* model for high

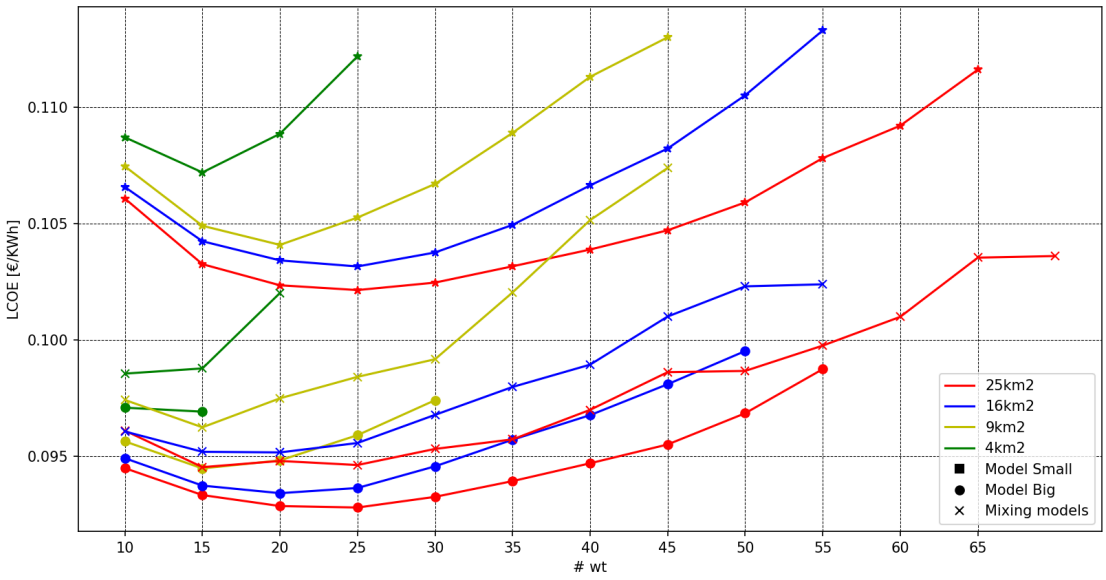

Figure 18: Optimal number of turbine for both models and in mixed configuration

numbers of wind turbines. This means that after a certain level of packing, the algorithm prefers the choice of smaller turbines at the cost of increasing the LCOE, because the choice of turbines of the larger model would result in a too packed configuration that would violate the penalties.

In fig. 19 one can appreciate the optimal disposition of the optimal number of turbines in the domain of $16km^2$ resulting from the optimization, that is 25 shown in fig. 18. The larger turbines are indicated in red and the smaller ones in gray.
As in the previous graphs, the map of the wind speed for the direction 310°, the prevailing wind direction, is presented.
From this graph one can better understand why the penalties have been defined as a circle of radius 1.5 times the diameter. By doing so, in fact, one guarantees the distance of three diameters if the turbines are of the same type. If, on the contrary, one is evaluating the distance between two turbines of different type, one has to consider that their diameter also varies, and therefore also the radius of the penalties, as shown in the figure by the dashed circumferences.

From the graph fig. 19 one can see how the optimal disposition tends to arrange along the diagonal of the domain. This phenomenon is particularly understandable by observing that it is a favorable configuration to the prevailing wind direction, allowing a greater number of turbines to catch it, despite the disadvantage in the directions that would see them aligned.

The configuration does not entail a particular advantage also considering that the turbines of type *Small* are 7, the minimum indispensable allowed by the penalties.

The fig. 20 represents the disposition of the optimal configuration, observed on the YZ plane so as to appreciate the difference in height between the different models of turbines.
The z plane on which it was decided to perform the section is the median plane of the turbines; that is, the one passing through the average value of the x positions of all the turbines present in the disposition.

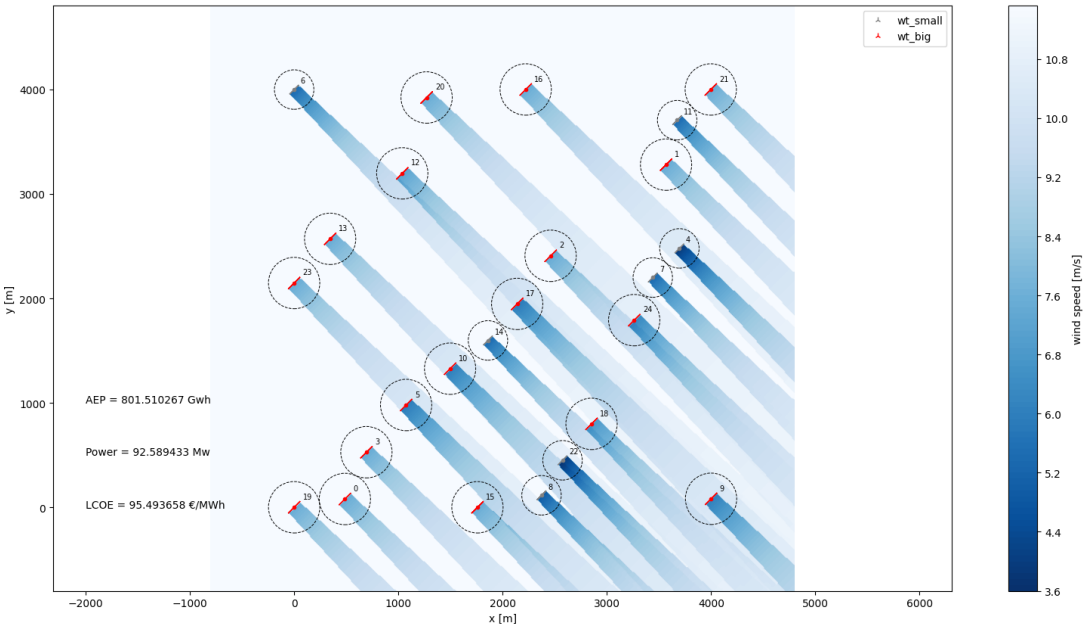

Figure 19: Optimal disposition for 25 wind turbines in mixing models configuration in a $16km^2$ domain

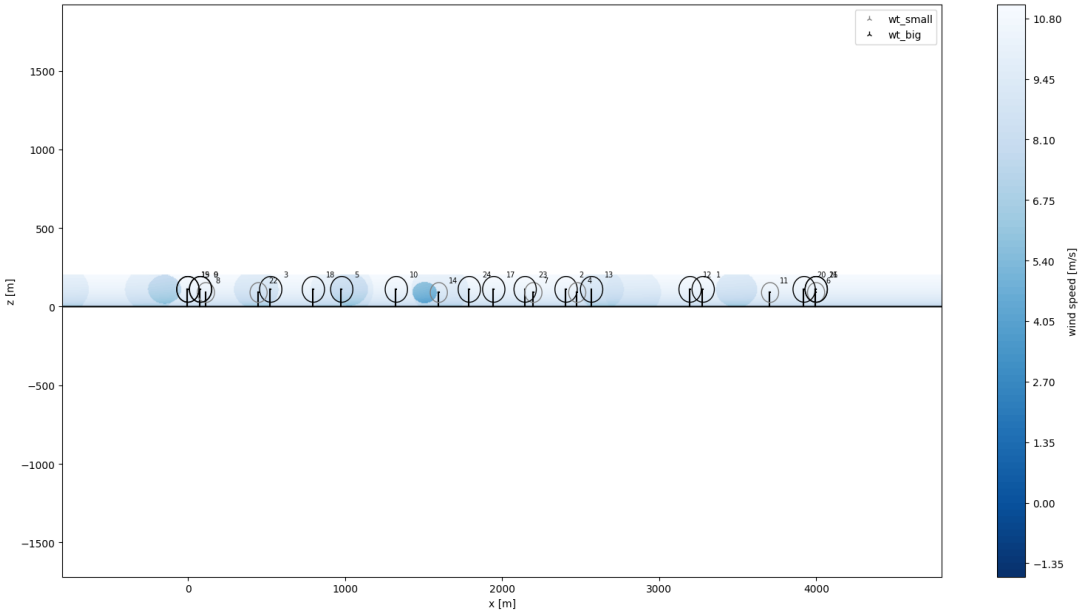

Figure 20: Optimal disposition for 20 wind turbines in mixing models Configuration, in YZ plan

5.2 Genetic algorithm Performance

The genetic algorithm is the factor that most affects the computation time. The convergence of the optimization of the layout requires a lot of time; in the order of hours.

The termination parameter of the solution, as discussed in section 4.1.3 is fixed a priori and depends exclusively on the number of generations and does not adapt to the performance of the algorithm itself.

The performance of the genetic algorithm, namely the convergence speed, depends strongly on the values of probability and shape of the probability curve for determining mutations and crossover.
During the preparation of the codes, best values for the specific simulation were searched for a long time. However, since they depend on many contingencies of the simulations, first of all the number of variables, and being the latter variable as in the case of the graph shown in section 5.1.1 in fig. 10, it was decided to use the default parameters offered by the Pymoo library as they perform better, at least in the specific case of the work of this thesis.

5.2.1 Parallelization

Besides working with the best values of η and *prob* for the probability distributions of crossover and mutations, another way to improve the computation times, where possible, is to parallelize the processes.

The operations that make up an algorithm are generally executed in a serial way; one after the other. However, where the algorithm allows it, the operations can be divided on the different cores that make up the computer, allowing to execute more operations at the same time. If these operations do not need the information obtained from each other and vice versa, the algorithm can be executed faster without compromising the result.
The improvement of the computation time is not precisely linear to the increase of the number of cores used; however, it is strongly influenced by it.

The algorithm used for the work of this thesis, as it was constituted, is predisposed for parallelization.
Specifically, the section in charge of genetic optimization consists of creating populations of individuals from generation to generation. The next generation is created based on the information obtained from the previous one; therefore the process must follow a linear order. On the contrary, however, what happens within the single generation does not follow this logic. In the generation, each individual is evaluated individually, independently of the others. This means that this part of the algorithm can be composed of calculations not performed simultaneously, therefore parallel.

The predisposition of the algorithm for parallel computing required considerable work.
In any case, the result of test simulations showed an effective parallelization of the code. However, the simulations in question for this thesis work, the search for the optimal number of wind turbines for a specific domain, require a computational effort that cannot be supported by a single core. This translates into a slowdown of the parallelization operations to wait for the remaining space needed to be freed on other cores. The conclusion of this is such an extension of the parallelization

times, as to nullify the benefits brought by this technique until extending the overall computation time in a non-negligible way.

For the final calculations, performed to obtain the results presented above presented, it was decided to use serial codes and not parallel ones.

6 Conclusion

The purpose of this thesis was to optimize the spatial arrangement of an array of floating off-shore wind turbines to increase their productivity and reduce the cost of energy production.

Given the definition of the problem, the analysis was carried out using an evolutionary optimization algorithm, being able to easily create a structure of individuals and generations.
An algorithm with statistical convergence requires to work with a large number of simulations, which implies that the aerodynamics analysis for the evaluation of the array performance must be carried out quickly, even introducing a greater error.
This is the context that led to the choice of combining a genetic optimization algorithm with a aerodynamics analysis algorithm, based on analytical relations. The latter have a lower computational cost than alternative models, and allow to increase the number of simulations, a quality necessary to obtain consistent results from an evolutionary algorithm.

The results for the analyses performed with a fixed turbine model have shown that the codes are able to give consistent results.
The data presented show the functioning of the evolutionary process; how the genetic algorithm shapes the arrangement of the wind turbines based on the characteristics of the site. and how the turbines with the highest productivity are the first to become part of the optimized arrangement. The results converge to realistic values and with the expected trends. They demonstrate the existence of an optimal number of wind turbines that depends on the size of the domain.

Expanding the analysis to configurations formed by more than one turbine model did not lead to conclusive results. The energy cost is a compromise between the energy costs produced with the use of different models separately. This demonstrates once again their consistency, without bringing a real additional contribution.

In this thesis work, despite aiming to create an optimization algorithm with low computational effort, the main obstacle was the high computing time that made it prohibitive to carry out further analyses or to detail the results more to increase their accuracy. This aspect does not compromise the validity of the work, as it fits into a context where, with alternative models such as *CFD* analyses, it would not have been possible to carry out this type of combined analysis.

A possible future development can be achieved by using instrumentation with higher computing power that will make the calculation times more manageable so that very accurate results can be obtained in relatively short times. This will allow to define with good approximation the macro-characteristics of a wind-farm in order to proceed to the more detailed *CFD* analyses only at a later stage, on arrangements already pre-optimized with a considerable saving of total time. For example, the specific positions of each wind turbine with a high-fidelity model, after having previously determined the optimal number of wind turbines with the model presented in this thesis.

As for the combination of different turbine models within the same wind-farm, a possible future development could be the implementation of the algorithms presented in this thesis with turbine models defined ad hoc. Adopting generators of equal power but arranged at very different heights from each other could lead to more optimized arrangements in productivity and therefore in energy costs, for the same domain.

This thesis can be considered as an example of combining two algorithms to create an optimizer

that was simple and with low computational effort. Moreover, it can be considered as a first step in the direction of finding advantageous the combination of two different types of turbines that exploit winds at different heights to optimize the use of a certain area. In both cases with the aim of reducing the cost of energy production. This is not only in the interest of the investor who sees his profits increase; it also makes the difference between an economically advantageous and an experimental energy source. In recent years, the reduction of this cost and the increase of those of fossil fuels, has opened the way for many alternative sources of energy, freeing them from a policy of subsidies. It has allowed them economic autonomy that has given them authority, reliability and a central role in the ecological transition process that the world is facing.
Optimizing productivity and cost of energy production for an energy source makes it more and more competitive and able to counter fossil fuels, notoriously cheap and polluting. And that's why I did this thesis; in the hope of bringing a small contribution to the research, with the aim of using what I learned in my studies to do my part, in the certainty of following the moral direction that I feel imposed by this historical period.

References

[1] BloombergNEF. *Global Low-Carbon Energy Technology Investment Surges Past $1 Trillion for the First Time*. URL: https://about.bnef.com/blog/global-low-carbon-energy-technology-investment-surges-past-1-trillion-for-the-first-time/.

[2] World Economic Formu. *The Future of Nature and Business*. URL: https://www3.weforum.org/docs/WEF_The_Future_Of_Nature_And_Business_2020.pdf.

[3] IPCC. *CLIMATE CHANGE 2014, Mitigation of Climate Change*. URL: https://www.ipcc.ch/site/assets/uploads/2018/03/WGIIIAR5_SPM_TS_Volume-3.pdf.

[4] Statista. *Net electricity consumption worldwide in select years from 1980 to 2021*. URL: https://www.statista.com/statistics/280704/world-power-consumption/#:~:text=Global%20electricity%20consumption%201980%2D2021&text=The%20world's%20electricity%20consumption%20has,increased%20by%20roughly%2075%20percent..

[5] Ember. *The transition from coal to clean*. URL: https://ember-climate.org/.

[6] Our world in data. *Share of electricity production by source, World*. URL: https://ourworldindata.org/grapher/share-elec-by-source.

[7] Ember. *Global Electricity Mid-Year Insights 2022*. URL: https://ember-climate.org/insights/research/global-electricity-mid-year-insights-2022/.

[8] EnerData. *Total energy consumption*. URL: https://yearbook.enerdata.net/total-energy/world-consumption-statistics.html.

[9] Statista. *Electricity consumption per capita worldwide in 2021, by selected country*. URL: https://www.statista.com/statistics/383633/worldwide-consumption-of-electricity-by-country/.

[10] EnerData. *Total energy consumption*. URL: https://yearbook.enerdata.net/total-energy/world-consumption-statistics.html.

[11] Worldometer. *Regions in the world by population (2023)*. URL: https://www.worldometers.info/world-population/population-by-region/.

[12] Worldometer. *Countries in the world by population (2023)*. URL: https://www.worldometers.info/world-population/population-by-country/.

[13] Wikipedia. *List of countries by carbon dioxide emissions*. URL: https://en.wikipedia.org/wiki/List_of_countries_by_carbon_dioxide_emissions.

[14] British International Investment. *Emerging Economies Climate Report 2022*. URL: https://www.bii.co.uk/en/news-insight/insight/articles/emerging-economies-climate-report-2022/.

[15] European Counsil. *Cambiamenti climatici: il contributo dell'UE*. URL: https://www.consilium.europa.eu/it/policies/climate-change/#2050.

[16] Consiglio Europeo. *Pronti per il* 55%. 2021. URL: https://www.consilium.europa.eu/it/policies/green-deal/fit-for-55-the-eu-plan-for-a-green-transition/.

[17] Consiglio dell'unione europea. *Il Consiglio e il Parlamento raggiungono un accordo provvisorio in merito alla direttiva sulla promozione delle energie rinnovabili*. URL: https://www.consilium.europa.eu/it/press/press-releases/2023/03/30/council-and-parliament-reach-provisional-deal-on-renewable-energy-directive/.

[18] Consiglio dell'unione europea. *"Pronti per il 55%": il Consiglio concorda obiettivi più ambiziosi per le energie rinnovabili e l'efficienza energetica*. URL: https://www.consilium.europa.eu/it/press/press-releases/2022/06/27/fit-for-55-council-agrees-on-higher-targets-for-renewables-and-energy-efficiency/.

[19] Consiglio dell'unione europea. *Infografica - Pronti per il 55%: come l'UE intende trattare le emissioni al di fuori del suo territorio*. URL: https://www.consilium.europa.eu/it/infographics/fit-for-55-cbam-carbon-border-adjustment-mechanism/.

[20] World Resource Institute. *10 Big Findings from the 2023 IPCC Report on Climate Change*. URL: https://www.wri.org/insights/2023-ipcc-ar6-synthesis-report-climate-change-findings.

[21] La Repubblica. *Da dove viene la nostra energia*. URL: https://www.repubblica.it/green-and-blue/2022/03/31/news/italia_energia_gas_petrolio_russia_italy_for_climate-341032602/.

[22] ISPRA. *L'andamento delle emissioni*. URL: https://www.isprambiente.gov.it/it/attivita/cambiamenti-climatici/landamento-delle-emissioni.

[23] IPCC. *Emissions Scenarios*. URL: https://www.ipcc.ch/report/emissions-scenarios/.

[24] IPCC. *Climate Change 2022: Impacts, Adaptation and Vulnerability*. URL: https://www.ipcc.ch/report/ar6/wg2/.

[25] Our World in Data. *Modern renewable energy generation by source, World*. URL: https://ourworldindata.org/grapher/modern-renewable-prod.

[26] IEA. *Renewables*. URL: https://www.iea.org/reports/global-energy-review-2020/renewables.

[27] Rinnovabili.it. *REN21: i record delle rinnovabili nel mondo sono oscurati dalle fossili*. URL: https://www.rinnovabili.it/energia/politiche-energetiche/rinnovabili-nel-mondo-record/.

[28] IRENA. *Renewable Energy Statistics 2021*. URL: https://www.irena.org/publications/2021/Aug/Renewable-energy-statistics-2021.

[29] Eni. *L'incessante forza del vento*. URL: https://www.eni.com/it-IT/innovazione-tecnologie/eolico.html.

[30] Wikipedia. *Energia eolica*. URL: https://it.wikipedia.org/wiki/Energia_eolica.

[31] Wikipedia. *Floating wind turbine*. URL: https://en.wikipedia.org/wiki/Floating_wind_turbine.

[32] DNV. *Floating Offshore Wind*. URL: https://www.dnv.com/focus-areas/floating-offshore-wind/index.html.

[33] Wikipedia. *Navier–Stokes equations*. URL: https://en.wikipedia.org/wiki/Navier%E2%80%93Stokes_equations.

[34] Ivar Øyvind Sand Anders Hallanger. *CFD Wake Modelling with a BEM Wind Turbine Sub-Model*. URL: https://www.mic-journal.no/ABS/MIC-2013-1-3.asp/.

[35] Matthew J. Churchfield Luis A. Mart´ınez-Tossas. *Large Eddy Simulation of wind turbine wakes: detailed comparisons of two codes focusing on effects of numerics and subgrid modeling*. URL: https://www.nrel.gov/docs/fy15osti/64912.pdf.

[36] Wikipedia. *Large eddy simulation*. URL: https://en.wikipedia.org/wiki/Large_eddy_simulation#Sub-grid_scale_models.

[37] Wikipedia. *Reynolds-averaged Navier–Stokes equations*. URL: https://en.wikipedia.org/wiki/Reynolds-averaged_Navier%E2%80%93Stokes_equations.

[38] Adil Rasheed Mandar Tabib. *LES and RANS simulation of onshore Bessaker wind farm: nalysing terrain and wake effects on wind farm performance*. URL: https://iopscience.iop.org/article/10.1088/1742-6596/625/1/012032/pdf.

[39] Jens Sørensen Søren Andersen. *Comparison of Engineering Wake Models with CFD Simulations*. URL: https://www.researchgate.net/publication/274908957_Comparison_of_Engineering_Wake_Models_with_CFD_Simulations.

[40] University of Notre Dame. *Wind Farm*. URL: https://www3.nd.edu/~tcorke/w.windturbinecourse/WindFarms_Presentation_a.pdf.

[41] N.O. Jensen. *A note on wind generator interaction*. URL: https://findit.dtu.dk/en/catalog/537f0cea7401dbcc120069bd.

[42] Tamás Bányai A. Bonanni. *Wind farm optimization based on CFD model of single wind turbine wake*. URL: https://www.researchgate.net/publication/289765117_Wind_farm_optimization_based_on_CFD_model_of_single_wind_turbine_wake.

[43] PyWake. *Engineering Wind Farm Models Object*. URL: https://topfarm.pages.windenergy.dtu.dk/PyWake/notebooks/EngineeringWindFarmModels.html#BastankhahGaussianDeficit.

[44] Fernando Porté-Agel Majid Bastankhah. *A new analytical model for wind-turbine wakes*. URL: https://www.sciencedirect.com/science/article/abs/pii/S0960148114000317.

[45] Wikipedia. *Artificial neural network*. URL: https://en.wikipedia.org/wiki/Artificial_neural_network.

[46] D.E.I.S. - Università di Bologna Daniele Vigo. *Algoritmi metaeuristici: I - introduzione*. URL: http://www.or.deis.unibo.it/didatt_pages/mmsd_ce/metaeuristici-I-introduzione%20rev20.pdf.

[47] Wikipedia. *Simulated annealing*. URL: https://en.wikipedia.org/wiki/Simulated_annealing.

[48] Wikipedia. *Ant colony optimization algorithms*. URL: https://en.wikipedia.org/wiki/Ant_colony_optimization_algorithms.

[49] Wikipedia. *Tabu search*. URL: https://en.wikipedia.org/wiki/Tabu_search.

[50] Pymoo. *GA: Genetic Algorithm*. URL: https://pymoo.org/algorithms/soo/ga.html#nb-ga.

[51] Wikipedia. *Multi-objective optimization*. URL: https://en.wikipedia.org/wiki/Multi-objective_optimization.

[52] Pymooo. *Sampling*. URL: https://pymoo.org/operators/sampling.html.

[53] Pymooo. *Selection*. URL: https://pymoo.org/operators/selection.html.

[54] Pymooo. *CrossOver*. URL: https://pymoo.org/operators/crossover.html.

[55] Yousaf Shad Muhammad Abid Hussain. *Trade-off between exploration and exploitation with genetic algorithm using a novel selection operator*. URL: https://link.springer.com/article/10.1007/s40747-019-0102-7.

[56] Wikipedia. *Genetic algorithm*. URL: https://en.wikipedia.org/wiki/Genetic_algorithm.

[57] Wikipedia. *Travelling salesman problem*. URL: https://en.wikipedia.org/wiki/Travelling_salesman_problem.

[58] Cornell University Jan Scholz. *Genetic Algorithms and the Traveling Salesman Problem a historical Review*. URL: https://arxiv.org/abs/1901.05737.

[59] Alexander Raul Meyer Forsting Niels Troldborg. *A simple model of the wind turbine induction zone derived from numerical simulations*. URL: https://onlinelibrary.wiley.com/doi/epdf/10.1002/we.2137.

[60] Ole Steen Rathmann. *The Park2 Wake Model - Documentation and Validation*. URL: https://backend.orbit.dtu.dk/ws/portalfiles/portal/151671395/Park2_Documentation_and_Validation.pdf.

[61] J Herna'ndez A. Crespo. *Turbulence characteristics in wind-turbine wakes*. URL: https://www.sciencedirect.com/science/article/abs/pii/016761059500033X.

[62] Gunner Chr. Larsen. *European wind turbine standards II (EWTS-II)*. URL: https://orbit.dtu.dk/en/publications/european-wind-turbine-standards-ii-ewts-ii.

[63] Sten Tronaes Frandsen. *Turbulence and turbulence-generated structural loading in wind turbine clusters*. URL: https://orbit.dtu.dk/en/publications/turbulence-and-turbulence-generated-structural-loading-in-wind-tu.

[64] Wen Zhong Shen Ju Feng. *Solving the wind farm layout optimization problem using random search algorithm*. URL: https://www.sciencedirect.com/science/article/abs/pii/S0960148115000129.

[65] Nicolai Gayle Nygaard. *A Turbulence Optimized Park model*. URL: https://github.com/OrstedRD/TurbOPark/blob/main/TurbOPark%20description.pdf.

[66] DTU Wind Energy. *DTU Wind Energy*. URL: https://github.com/DTUWindEnergy/PyWake/blob/master/py_wake/ground_models/ground_models.py.

[67] ABB. *Quaderni di applicazione tecnica N.13. Impianti eolici*. URL: https://www.docenti.unina.it/webdocenti-be/allegati/materiale-didattico/548395.

[68] National Renewable Energy Laboratory. *turbine-models*. URL: https://github.com/NREL/turbine-models.

[69] drømstørre. *The Power Curve of a Wind Turbine*. URL: http://xn--drmstrre-64ad.dk/wp-content/wind/miller/windpower%20web/en/tour/wres/pwr.htm.

[70] Wikipedia. *Betz's law*. URL: https://en.wikipedia.org/wiki/Betz%27s_law.

[71] PyWake Documentation. *Wind Turbine Object*. URL: https://topfarm.pages.windenergy.dtu.dk/PyWake/notebooks/WindTurbines.html.

[72] LIFES50+. *Qualification of innovative floating substructures for 10MW wind turbines and water depths greater than 50m. Deliverable 2.8 Expected LCOE for floating wind turbines 10MW+ for 50m+ water depth*. URL: https://ec.europa.eu/research/participants/documents/downloadPublic?documentIds=080166e5c3ac71f4&appId=PPGMS.

[73] Catho Bjerkseter Anders Myhr. *Levelised cost of energy for offshore floating wind turbines in a life cycle perspective*. URL: https://reader.elsevier.com/reader/sd/pii/S0960148114000469?token=693CF7A4A3A314C36269BB31189DBD7E772D2666915DA137828CBB5E6630A6originRegion=eu-west-1&originCreation=20230421161529.

[74] *Usability first: scientific visualization definition*. 2011. URL: https://guidetoanoffshorewindfarm.com/lifecycle#1.

[75] Christopher Neil Elkinton. *Offshore wind farm layout optimization*. URL: https://scholarworks.umass.edu/dissertations/AAI3289248/.

[76] J. Carlos Alvarez Laura Castro-Santos. *Influence of the Discount Rate in the Economic Analysis of a Floating Offshore Wind Farm in the Galician Region of the European Atlantic Area*. URL: https://www.researchgate.net/publication/327875551_Influence_of_the_Discount_Rate_in_the_Economic_Analysis_of_a_Floating_Offshore_Wind_Farm_in_the_Galician_Region_of_the_European_Atlantic_Area.

[77] IEA. *Projected Costs of Generating Electricity 2020*. URL: https://www.iea.org/reports/projected-costs-of-generating-electricity-2020.

[78] Life +50. *Qualification of innovative floating substructures for 10MW wind turbines and water depths greater than 50m. Deliverable 2.2. LCOE tool description, technical and environmental impact evaluation procedure*. URL: https://lifes50plus.eu/wp-content/uploads/2016/10/GA_640741_D2.2-internal.pdf.

[79] The Carbon Trust. *Floating Offshore Wind: Market and Technology Review*. URL: https://ctprodstorageaccountp.blob.core.windows.net/prod-drupal-files/documents/resource/public/Floating%20Offshore%20Wind%20Market%20Technology%20Review%20-%20REPORT.pdf.

[80] Fergus Sharkey. *Off-shor Electrical Networks and Grid Integration of Wave Energy Converter Arrays - Techno-economic Optimisation of Array Electrical Networks, Power Quality Assessment, and Irish Market Perspectives*. URL: https://arrow.tudublin.ie/cgi/viewcontent.cgi?article=1078&context=engdoc.

[81] Anup J. Nambiar Adam J. Collin. *Electrical Components for Marine Renewable Energy Arrays: A Techno-Economic Review*. URL: https://www.mdpi.com/1996-1073/10/12/1973/pdf?version=1511873797&__cf_chl_tk=AFa0tKOQfGRl2Ol7xr6Jzq1xFXxNPX4HymrSchVUCYM-1682092728-0-gaNycGzNDjs.

[82] Rembrandt Koppelaar Elise Dupont a. *Global available wind energy with physical and energy return on investment constraints*. URL: https://www.sciencedirect.com/science/article/abs/pii/S0306261917313673.

Ringraziamenti

Grazie a tutti. Grazie ai miei relatori, grazie alla mia famiglia e grazie ai miei amici.
Grazie a tutti.